

University of Massachusetts Amherst
ScholarWorks@UMass Amherst

Masters Theses 1911 - February 2014

2012

Semi-Active Damping for an Intelligent Adaptive Ankle Prosthesis

Andrew K. Lapre

University of Massachusetts Amherst

Follow this and additional works at: <https://scholarworks.umass.edu/theses>



Part of the [Acoustics, Dynamics, and Controls Commons](#), [Applied Mechanics Commons](#), [Biomechanical Engineering Commons](#), [Biomechanics Commons](#), [Computer-Aided Engineering and Design Commons](#), and the [Electro-Mechanical Systems Commons](#)

Lapre, Andrew K., "Semi-Active Damping for an Intelligent Adaptive Ankle Prosthesis" (2012). *Masters Theses 1911 - February 2014*. 805.

Retrieved from <https://scholarworks.umass.edu/theses/805>

This thesis is brought to you for free and open access by ScholarWorks@UMass Amherst. It has been accepted for inclusion in Masters Theses 1911 - February 2014 by an authorized administrator of ScholarWorks@UMass Amherst. For more information, please contact scholarworks@library.umass.edu.

**SEMI-ACTIVE DAMPING FOR AN INTELLIGENT ADAPTIVE ANKLE
PROSTHESIS**

A Thesis Presented

by

ANDREW KENNEDY LAPRE

Submitted to the Graduate School of the
University of Massachusetts Amherst in partial fulfillment
of the requirements for the degree of

MASTER OF SCIENCE IN MECHANICAL ENGINEERING

May 2012

Department of Mechanical and Industrial Engineering

© Copyright by Andrew Kennedy LaPrè 2012

All Rights Reserved

**SEMI-ACTIVE DAMPING FOR AN INTELLIGENT ADAPTIVE ANKLE
PROSTHESIS**

A Thesis Presented

by

ANDREW KENNEDY LAPRE

Approved as to style and content by:

Frank C Sup, Chair

Yossi Chait, Member

Joseph Hamill, Member

Donald Fisher, Department Head
Department of Mechanical and Industrial
Engineering

DEDICATION

I would like to dedicate this thesis to my parents Maribeth and Robert LaPrè. They have been an incredible source of support throughout the years, demonstrating the value of hard work, and encouraging me to not only reach for my goals, but to do everything morally possible to achieve the success I strive for. Without them it would have been a long shot for me to attain this degree.

ACKNOWLEDGMENTS

I would like to thank my advisor, Professor Frank Sup, for all of his support, guidance, and encouragement throughout my time working for him as a graduate student. He has been an invaluable asset to my continued education of mechatronics and robotics outside of the classroom, as well as a great source of inspiration and motivation that I will take with me well past my days as a student. I'd also like to thank the members of my committee, Profs Yossi Chait and Joseph Hamill for their feedback and contributions to my thesis project. They too have been a great source of inspiration, guidance and knowledge throughout my years as a student.

Thank you to everyone I've worked with in the Mechatronics and Robotics Research Laboratory and the Kinesiology Biomechanics Laboratory. Lastly, thank you to all of my terrific friends in the Mechanical and Industrial Engineering Department who have supported me and made the University of Massachusetts Amherst such a fun and pleasant place to work.

ABSTRACT

SEMI-ACTIVE DAMPING FOR AN INTELLIGENT TERRAIN ADAPTIVE ANKLE PROSTHESIS

MAY 2012

ANDREW KENNEDY LAPRE, B.S., UNIVERSITY OF MASSACHUSETTS

M.S.M.E., UNIVERSITY OF MASSACHUSETTS AMHERST

Directed by: Professor Frank Sup

Modern lower limb prostheses are devices that replace missing limbs, making it possible for lower limb amputees to walk again. Most commercially available prosthetic limbs lack intelligence and passive adaptive capabilities, and none available can adapt on a step by step basis. Often, amputees experience a loss of terrain adaptability as well as stability, leaving the amputee with a severely altered gait. This work is focused on the development of a semi-active damping system for use in intelligent terrain adaptive ankle prostheses. The system designed consists of an optimized hydraulic cylinder with an electronic servo valve which throttles the hydraulic fluid flowing between the cylinder's chambers, acting on the prosthesis joint with a moment arm in series with a carbon spring foot. This provides the capability to absorb energy during the amputees gait cycle in a controlled manner, effectively allowing the passive dynamic response to be greatly altered continuously by leveraging a small energy source. A virtual simulation of an amputee gait cycle with the adaptive semi-active ankle design revealed the potential to replicate adaptive abilities of the human ankle. The results showed very similarly that irregularities in amputee biomechanics can be greatly compensated for using semi-active damping.

TABLE OF CONTENTS

	Page
ACKNOWLEDGMENTS	v
ABSTRACT.....	vi
TABLE OF TABLES	ix
TABLE OF FIGURES.....	x
CHAPTER	
1 THESIS OBJECTIVE	1
1.1 Research Objective.....	1
1.2 Research Approach	2
1.3 Scope	3
1.4 Thesis Layout	3
2 BACKGROUND.....	5
2.1 Damping Technology	5
2.2 Current Ankle/Foot Prosthesis Technology	6
2.3 Ankle Biomechanics	8
3 SIMULATION OF A SLOPE ADAPTING ANKLE PROSTHESIS PROVIDED BY SEMI-ACTIVE DAMPING	11
3.1 Introduction	11
3.2 Model	14

3.3	Data Collection.....	15
3.4	Methodology	21
3.5	Results and Discussion.....	23
4	A SEMI-ACTIVE DAMPING DESIGN FOR USE IN A TERRAIN ADAPTIVE ANKLE PROSTHESIS	26
4.1	Introduction	26
4.2	Prior Works	29
4.3	Damper Design.....	30
4.4	Test Bed Design	37
4.5	Simulated Results	39
4.6	Post Publication Design Changes.....	40
5	CHARACTERIZATION/TESTING OF THE SEMI-ACTIVE DAMPING SYSTEM	42
5.1	Introduction	42
5.2	Prior Works	46
5.3	Hardware Simulation Test Bed	47
5.4	Methods and Results	50
5.4.1	Characterization	50
5.4.2	Hardware in the Loop Simulation.....	55
5.5	Conclusion.....	58
6	THESIS CONTRIBUTIONS AND RECOMMENDATIONS	59
	BIBLIOGRAPHY	64

LIST OF TABLES

TABLE	Page
1. Subject description.....	16
2. Marker placement	18
3. Damping coefficient (N-m-s/deg) updates at different events.....	23
4. Design parameters constraints and performance criteria	31
5. Design requirements for linear foot hardware	48
6. Exponential fit coefficients for positive and negative velocities.	51
7. Average foot and locked damper stiffness used in hardware simulation.....	55

LIST OF FIGURES

Figure	Page
1. A hydraulic representation of passive, semi-active and active damping showing their damping coefficient b ranges while in operation.	6
2. A SACH foot, Solid Ankle Cushioned Heel (left), and carbon fiber spring foot (right).	7
3. Two commercially available terrain adaptive prostheses, Endolite Echelon (left) and Ossur Proprio (right).	8
4. Gait cycle for normal human walking with -15%, 0%, and 15% slope shown for able-bodied persons as the solid lines [7], and 0% slope shown for a unilateral transtibial amputee shown as a dashed line [8].	9
5. Normal human biomechanics divided into phases, and sub phases [9].	10
6. Spring-damper model representing a carbon-fiber foot, k_f , in series with a modulated damper, b , and return spring, k_r in the linear domain (left) and rotational domain (right).	14
7. Experimental setup showing subject knowingly stepping onto an altered terrain at a self-selected pace while ground reaction forces and limb trajectories are recorded.	17
8. Model created from a standing calibration file, used to calculate biomechanics data from movement files with calibration and tracking markers shown.	20
9. MATLAB Simulink model used to simulate the addition of a damper in series with the carbon spring foot from the biomechanics data recorded.	21
10. Identifiable gait events that mark the changes in the damping coefficient shown on an example adaptive ankle angle plot.	22
11. Adaptive ankle simulation compared with the subject's passive spring foot/ankle and able bodied data[22] on level ground and ten-degree inclines and declines.	24
12. Ankle power of able-bodied and transtibial amputee during self-selected speed walking showing 0%, +15%, and -15% slope data for able bodied persons [7], and 0% slope for transtibial amputees using passive prostheses [8].	27
13. Spring-damper model representing a carbon-fiber foot with stiffness k_f , in series with a modulated damper with variable damping coefficient b , and return spring with stiffness k_r in the	

linear domain (left) and rotational domain (right). In the linear domain, damper displacement is noted as x_1 , and foot flexion is denoted as x_2 . In the rotational domain, they are denoted as θ_d and θ_f .	28
14. Cylinder optimization surface response with inner radius and moment arm as design parameters shown with the maximum allowable working pressure nonlinear constraint.	32
15. Simulated damper flow rates for the adaptive ankle prosthesis during level and sloped walking.	33
16. Damper assembly (left) and exploded view (right).	36
17. Damper shown installed in an adaptive ankle prosthesis prototype.	37
18. Damper test bench shown with key components labeled.	38
19. Simulation of the adaptive ankle which takes inputs of existing amputee prosthesis ankle torque data and outputs the simulated ankle angle, compared with the passive ankle prosthesis data and able-bodied data [7], for stepping on a ten-degree decline from a level surface.	40
20. Adaptive ankle concept shown in linear domain (left) and rotational domain (right) consisting of a spring foot with stiffness k_{foot} in series with variable damper b and return spring with stiffness k_{return} in parallel.	44
21. First generation fabricated damper and servo-valve used for control development.	45
22. Linear foot spring mechanism having independent stiffness values for plantar flexion and dorsiflexion in the linear domain.	48
23. Test bed shown with key assemblies labeled.	49
24. Damping coefficient in the tunable range for positive and negative velocities show with exponential fits.	51
25. Recorded Exlar linear actuator position, actuator velocity, exerted force, damper position from top to bottom for damper and linear foot stiffness calculations.	52
26. Damper position vs system force.	53
27. Loading and unloading phases for positive and negative displacement loading conditions for locked damper condition stiffness calculation.	53

28. Linear foot deflection vs system force for foot stiffness calculations.	54
29. Loading and unloading phases for positive and negative displacement loading conditions for linear foot stiffness calculation.	54
30. Ankle torque and angle for different initial steps showing the hybrid hardware in the loop adaptive simulation compared to able-bodied and passive amputee biomechanics data.....	57
31. CAD model of dynamic joint impedance testing robot design.....	61
32. Close up of dynamic joint impedance testing robot.....	62

CHAPTER 1

THESIS OBJECTIVE

Ankle-foot prostheses restore the walking ability to lower limb amputees. Great strides have been made in replacing the lost limb, but current prosthetic technology still limits the capabilities and activities that amputees are able to perform. Everyday activities such as walking up or down a hill, or ascending or descending stairs, can prove to be very challenging for a lower limb amputee. In addition, when unintended events occur such as stepping on a rock or curb, maintaining ones balance and stability may be impossible.

Recent advances in robotics make possible the development of a prosthesis that can act as an extension of oneself. By also making the control of the device intuitive, the amputee needs to worry less about its operation and can be more concerned about participating in activities of daily life. If a device can detect changes in the ground and automatically adjust to both expected and unexpected disturbances, the difficulties amputees face when ambulating varied terrains can be overcome.

1.1 Research Objective

The objective of this research is to develop a semi-active damping system for use in ankle prostheses. Semi-active damping will give passive prostheses the ability to adapt to changing terrain by modifying the systems dynamic parameters.. As a result, the development of this technology will provide a measure of stability not obtainable in currently available lower limb passive prostheses. The effect of the prosthesis will be to minimize falls and increase the user's confidence.

1.2 Research Approach

In order to overcome challenges stated in Section 1.2 and meet the objective outcome of this research, the project has been divided into three parts, of which the first two have already been implemented and published in refereed conference proceedings, and the third is in the process of being accepted for publishing. The research approach is as follows, each addressing specific engineering challenges.

The first phase of the project was to identify the performance of a healthy human ankle and current commercial passive prostheses. This allowed a comparison that highlights the performance needs of the semi-active damping system designed. In order to accomplish this task, a biomechanics study was performed recording both able-bodied and transtibial gait cycles, followed by a data analysis and simulation of the proposed solution.

The second phase of the project was the design and fabrication of both the semi-active damping system to be used as a prototype, and test bed apparatus that will be essential for developing control algorithms needed to control the semi-active damping. This was accomplished using standard mechanical engineering practices, using the biomechanics data collected in the prior phase for design specifications.

The third phase involved the development of control strategies for the damping system in the test bed apparatus, and documenting the results. A novel control strategy had to be developed since the system's passive dynamics change throughout the gait cycle.

Dividing the research into these sections will result in benefits that aid more than just the progress of this research progress. This helps to further the existing knowledge and progress in academia as a whole. It also helps to keep the project focused and continually in a forward direction which is important for the projects successful completion. The long term benefits of

this research is the construction of a platform to base a new succession of intelligent, intuitive prostheses, and possibly even other robotic devices where environmentally adaptive stability is needed.

1.3 Scope

Designing an intelligent adaptive ankle prosthesis poses a challenging research focus, which involves the coordination of many tasks and attaining the help from many people in order to meet the final goal. It is funded by the Mechatronics and Robotics Research Laboratory at the University of Massachusetts, and directed by Professor Frank Sup. Also involved is Dr Hamill of the Kinesiology Department at the University of Massachusetts for direction in the field of biomechanics. The project deliverables include three publications, documentation of the entire project, and a semi-active damper prototype design with a state of the art control method. The project ends leading into future work building and testing the prosthesis prototype, and a redesign to bring the device to a level where it can be commercialized.

1.4 Thesis Layout

The format of this thesis is an adaptation from a collection of papers on the development of the adaptive ankle prosthesis. After the first chapter which introduces the project, a brief overview of three concepts will be presented so that information detailed in the later chapters will be comprehensible to the reader. These concepts are damping, current ankle/foot prosthesis technology, and ankle biomechanics.

The third chapter presents the findings reported in a recent paper “Simulation of a Slope Adapting Ankle Prosthesis Provided by Semi-Active Damping” that has been published as a technical paper in the proceedings of Engineering in Medicine and Biology Conference 2011 [1]. This paper covers the mathematical modeling of the prosthesis, collection of amputee

biomechanics data on changing terrains, and a MATLAB simulation of the adaptive prosthetic ankle. The results are compared to the biomechanics data of the amputee data using their daily-use prosthesis, and healthy biomechanics from the literature. The chapter goes more into depth with the information presented in the publication, showing more specifically the process of the data collection, results, and how the results were obtained. It concludes with a discussion about the results, what they mean, and leads into what the next steps of the project are.

Chapter four is the presentation of the design presented in the second publication “A Semi-Active Damper Design for Use in a Terrain Adaptive Prosthetic Ankle” that has been published as a technical paper in the proceedings of the International Mechanical Engineering Congress and Exposition [2]. This paper covers the design process, final design and testing strategies of the damper discussed in the second and third chapters. A prototype of the adaptive ankle prosthesis is introduced as well. This paper ends with a brief overview of design changes that were made post-publication.

Chapter five presents the characterization and testing of the system. Testing procedures and results of the damper characterization are presented with the physical simulation of the damper inputting force and position trajectories and recording the dampers response as it adjusts.

The final chapter discusses what has been accomplished at this point. It highlights the important findings, including what needs to be changed and what studies need to be conducted in order to bring this project to the next step, which is a redesign of the damping system, retesting, and implementation in a tethered prototype. It concludes with the future direction of this project and steps beyond this thesis needed to bring the device to the level required for commercialization.

CHAPTER 2

BACKGROUND

This is an interdisciplinary project that involves many areas of understanding other than strictly mechanical engineering. This includes kinesiology for the understanding for normal human kinematics, electrical engineering for circuit design and the communication between mechanical and electrical systems, and some computer science to interface sensors to computers for data collection, control, and computation. To better understand this interdisciplinary work, a basic background of three areas will be covered: damping technology, current available prosthesis technology, and the healthy biomechanics of the human ankle.

2.1 Damping Technology

Damping is the process of removing mechanical energy from a system and transforming it into another type of energy (typically heat). Damping is usually done passively, which requires no external energy source, and doesn't store mechanical energy as other passive elements such as a spring would. The two main types of damping used to dissipate mechanical energy are coulomb friction, and viscous damping. Ideal kinetic coulomb friction creates a constant resistive force that is independent to the velocity at which the damping device is moving, once it is past the point of static friction and motion exists. Ideal viscous damping creates a resistive force that is proportional to the velocity at which the damper is moving.

Three types of viscous damping technology are involved with the current development of prosthetics: passive constant damping, semi-active damping, and active damping. Hydraulic versions of these can be seen in figure 1. Passive constant damping requires no external energy source to dissipate the mechanical energy, and has a constant positive damping coefficient. Semi-active damping requires a small external energy source to modulate the damping

coefficient, which can theoretically take a positive value between zero and infinity. A positive damping coefficient indicates energy dissipation. Active damping requires a large energy source to modulate the damping coefficient, which can theoretically take any value between negative and positive infinity. With active damping, the damper effectively becomes an actuator that can inject power into the system when the damping coefficient is negative, as well as dissipate energy when the damping coefficient is positive.

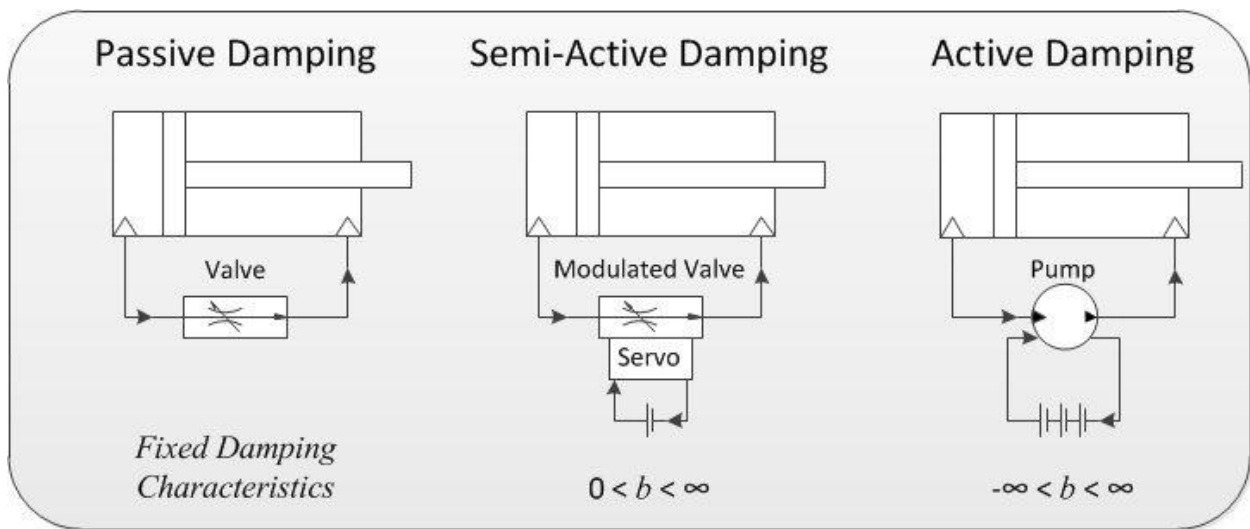


Figure 1. A hydraulic representation of passive, semi-active and active damping showing their damping coefficient b ranges while in operation.

2.2 Current Ankle/Foot Prosthesis Technology

Current prosthesis technology limits most amputees to completely passive devices. There are active devices being developed; however the relatively new emergence of robotic technologies makes these devices reliant on large batteries and motors that are capable of restoring biomechanically normal torques and powers to the ankle. There are two standard

options available to amputees. The SACH—Solid Ankle Cushioned Heel—and the carbon fiber spring feet are seen in figure 2.

The SACH foot is a wooden prosthesis with a rubber outer cover. It allows the amputee to ambulate however it offers little to help restore a normal gait pattern. There is no flexion at all, and can't conform to the ground on any terrain, resulting in a “roll over” walking method. Point contact is the biggest problem with this prosthesis, which results in many moments of instability.



Figure 2. A SACH foot, Solid Ankle Cushioned Heel (left), and carbon fiber spring foot (right).

The carbon fiber spring foot is the next evolution beyond the SACH foot. This type of prosthesis is flexible, allowing it to conform to the ground. It is optimized for level ground walking, storing energy after heel-strike, that is released during push off. This restores the users gait partially, however the fixed relationship between angular flexion and torque prevents the device from having stability during circumstances other than level ground walking.

There are newer devices that have recently been developed that provide a more natural gait by offering adaptation to the ground. The most notable of these devices are the Endolite Echelon and the Ossur Proprio Foot seen in figure 3. The Echelon incorporates passive damping

that has fixed damping rates for both dorsiflexion and plantar flexion. This allows the foot to conform to the terrain when walking up and down slopes, increasing stability. The damping rates are fixed however limiting the adaptation capabilities. The Proprio is the only passive prosthesis incorporating a microcontroller, and can adjust the neutral position of the spring foot during the swing phase of the gait cycle over a series of steps. The downside of this device is that there is no damping, and the controller assumes that the next step will have the same characteristics as the previous. This prevents adaptation on a step by step basis.



Figure 3. Two commercially available terrain adaptive prostheses, Endolite Echelon (left) and Ossur Proprio (right).

2.3 Ankle Biomechanics

The normal human walking gait cycle for walking on level ground and on inclined and declined slopes of 15 percent grades compared to level ground unilateral amputee gait can be seen in figure 4. The normal walking cycle is defined as starting and ending at the instant of heel strike [3], [4]. The cycle can be divided into the stance phase (the first 60% of the cycle), and the swing phase (SP) when the foot is off the ground (the final 40% of the cycle). The stance phase can be also divided into three sub-phases [5], [6]. These sub-phases consist of Controlled Plantarflexion, Controlled Dorsiflexion, and Powered Plantarflexion, seen in figure 5.

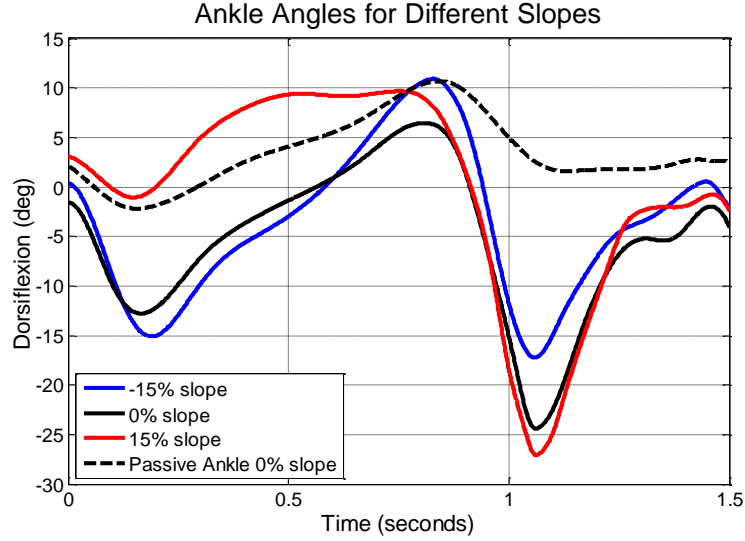


Figure 4. Gait cycle for normal human walking with -15%, 0%, and 15% slope shown for able-bodied persons as the solid lines [7], and 0% slope shown for a unilateral transtibial amputee shown as a dashed line [8].

Controlled Plantarflexion (CP) is the sub-phase in which the heel first touches the ground during heel strike, and controlled damping occurs until the foot is flat. Footflat can be seen at the local minima of the ankle angle portion of figure 4 during the first 0.5 seconds of the cycle. At this point the ankle velocity changes direction. During this phase, the ankle torque is directly proportional to the ankle angle. Also, net power is negative throughout this sub-phase, meaning power is being dissipated [5], [6].

Controlled Dorsiflexion (CD) is the sub-phase that starts at footflat and ends at maximum dorsiflexion. This can be seen at the maximum ankle angle in figure 4. During this stage, energy is stored in the ankle and foot, and ankle stiffness increases nonlinearly. There is usually a burst of positive power towards the end of this phase, which lasts for about the final 5% of CD [5], [6].

Powered Plantarflexion (PP) starts at maximum dorsiflexion, and ends at toe-off when the foot leaves the ground. Since net positive work is generated by able-bodied persons in this sub-phase, the performance of this phase will not be able to be matched by a passive prosthesis.

The most that can be expected is the return of a small amount of energy that is stored in the foot while flexing during CD [5], [6].

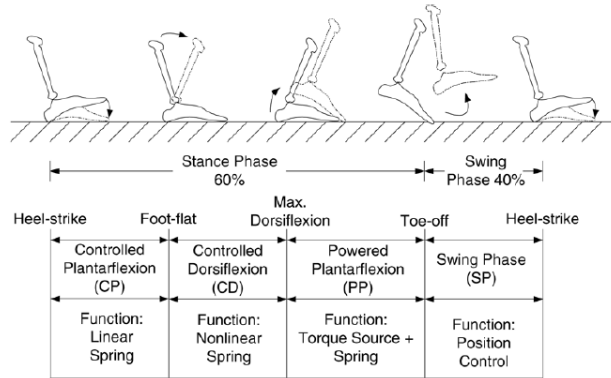


Figure 5. Normal human biomechanics divided into phases, and sub phases [9].

Using biomechanics data from Winter and Lay [7], [8] the target performance of the semi-passive ankle prosthesis has been specified. Power is negative because the triceps surae muscles are acting eccentrically during the first two phases. Since power is being dissipated during the first two sub-phases of the stance phase, it is concluded that it is possible to exactly replicate the performance of healthy able-bodied biomechanics with a passive device, so-long as the stiffness can be modulated. This will provide stable ground contact for the support of the load from the user. During what would normally be the controlled dorsiflexion sub-phase, it will be necessary to increase the impedance of the ankle preventing plantar flexion during roll-over since power will not be able to be generated with our semi-active damping device. During the swing phase of an able-bodied human, there is human anticipation which will influence the position that the ankle returns to when the foot is off of the ground [10], [11]. For the semi-active damping prosthesis, when the device is completely off of the ground, the device will return to the an acceptable position since it can't detect what the terrain is until ground contact has been made. The above describes the expected performance of the semi-active damping ankle prosthesis being designed.

CHAPTER 3

SIMULATION OF A SLOPE ADAPTING ANKLE PROSTHESIS PROVIDED BY SEMI-ACTIVE DAMPING

Adapted from a Technical Paper published in the *Proceedings of the 2011 International Conference of the IEEE Engineering in Medicine and Biology Society* [1]

Abstract— Modern passive prosthetic foot/ankles cannot adapt to variations in ground slope. The lack of active adaptation significantly compromises an amputee's balance and stability on uneven terrains. To address this deficit, this paper proposes an ankle prosthesis that uses semi-active damping as a mechanism to provide active slope adaptation. The conceptual ankle prosthesis consists of a modulated damper in series with a spring foot that allows the foot to conform to the angle of the surface in the sagittal plane. In support of this approach, biomechanics data are presented showing unilateral transtibial amputees stepping on a wedge with their daily-use passive prosthesis. Based on these data, a simulation of the ankle prosthesis with semi-active damping is developed. The model shows the kinematic adaptation of the prosthesis to sudden changes in ground slope. The results show the potential of an ankle prosthesis with semi-active damping to actively adapt to the ground slope at each step.

3.1 Introduction

Commercial passive prostheses currently available to lower limb amputees are optimized for level ground walking [12]. In these devices, the foot and ankle are replaced with a fixed carbon fiber spring that cannot adapt to variations in terrain or the user's activity (such as walking on slopes, descending and ascending stairs, and while standing up from a seated position). These activities can be accomplished, however only with the compensation of the other joints and extremities. A fixed, stiff ankle can create potentially unsafe conditions for

amputees, especially if there is a sudden or unexpected disturbance such as stepping on a rock or curb [13-15]. Studies have shown that the falling incidence rate in the amputee population is equal to that of institutionalized elderly, and about one out of ten lower limb amputees have reported requiring medical attention for a fall that has occurred within the year [16]. A significant limitation of passive ankle prostheses is that their range of motion is directly coupled to the ankle moment through the spring foot. This hinders an amputee's ability to maintain stable (foot flat) ground contact on uneven terrains. Resulting in a significant decrease in the walking stability of an amputee compared to an able-bodied person while walking on slopes [13]. In order to increase the stability of the amputee, an ideal prosthetic ankle would adapt to the terrain at each and every step.

To study the first step response to a new ground slope, able-bodied persons were studied during their initial step onto an inclined surface (called “wedge stepping”) [4]. This wedge stepping study focused on the biomechanics of the lower limbs and postural changes during the adaptation phase of gait. While no similar amputee wedge-stepping study was found in the literature, a study was conducted that focused on steady-state inclined walking of lower limb amputees [14]. The study clearly shows that an amputee's hip, knee, and sound ankle trajectories significantly compensate for both the kinematic and kinetic limitations of the ankle when walking up and down slopes [14].

The first attempt to address the adaptive deficiencies in prosthetic ankles was by Hans Mauch from the 1950s through the 1970s [17]. His passive ankle incorporated a hydraulic damper that allowed the ankle to adapt to the ground slope. It also featured a spring to return the foot to a neutral position after toe-off. The device demonstrated the potential of ankle adaptation, but mechanical failures prevented the device from being commercialized. Inspired by Mauch, a

friction-based device that adapts to sloped surfaces at heel strike and then locks as the device bears weight was developed at Northwestern University [18]. Commercially available, the Endolite Echelon foot/ankle is a passive hydraulic prosthesis with independent plantarflexion and dorsiflexion damping values that must be manually set. The prosthesis aims to passively mimic the visco-elastic response of human muscle with fixed damping and spring constants to provide ankle adaptation on sloped surfaces. Another commercial device, the Ossur Proprio Foot, is an electromechanical prosthesis. Using the onboard sensors, its control algorithm adapts incrementally by estimating the ground angle of the current step and then adjusts the ankle during swing assuming the next step will be on the same ground slope. The design of the Proprio Foot only allows for ankle adjustments while not bearing weight.

Powered active prostheses have been developed to deliver human-scale torque and power with an actuator [19-21]. Collectively these robotic devices demonstrate the potential to create intelligent prostheses using robotic technology that has only recently become available. The ability for these devices to enable step-by-step adaption is complicated by the advantage they offer (i.e. their ability to act in a forceful manner). This requires more detailed knowledge of the terrain and user's activity to coordinate the prosthesis with the user so as not to destabilize the amputee.

Of the above passive prostheses, none modulate the ankle's impedance in real-time to improve the adaptive behavior of the ankle. The semi-active damping approach presented in this paper modulates the behavior of the ankle in real-time based on the characteristics of the forceful interaction between the ground, prosthesis, and amputee that encode the changes in terrain and user's activity. In this manner, a semi-active approach provides the advantages of a fully active system, but relies on the user-prosthesis interaction to enhance an amputee's stability throughout

the gait cycle. In this paper, the biomechanics of transtibial amputees' first step onto ten-degree inclined and declined slopes from a level surface are studied. Based on these data, a model of an adaptive ankle comprising of a spring foot in series with an adjustable damper is presented. Simulation results show that such a device would be capable of effectively adapting to changes in ground slope in the sagittal plane. This work will provide a basis for future development of an adaptive ankle prosthesis that uses a semi-active damper to adapt to the ground slope at each step.

3.2 Model

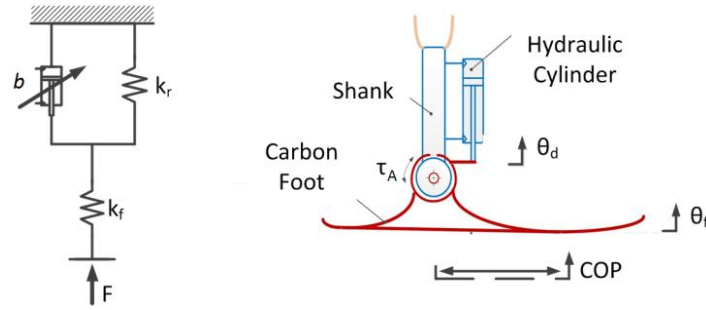


Figure 6. Spring-damper model representing a carbon-fiber foot, k_f , in series with a modulated damper, b , and return spring, k_r in the linear domain (left) and rotational domain (right).

The adaptive ankle model, figure 6, places the stiff spring foot, k_f , in series with a semi-active damper, b . In this model, the effective ankle angle is the summation of the deflection of the spring foot given by:

$$\theta_A = \theta_f + \theta_d \quad (3.1)$$

θ_f , θ_d , and θ_A are the carbon foot angular flexion, damper angle, and total ankle angle, respectively. In this configuration the net motion of the ankle is augmented by the damper element that is driven by the force transmitted by the spring foot. To modulate the damping coefficient in real-time, the system leverages semi-active damping to optimize the adaptation

throughout the gait cycle. In hydraulic semi-active damping, the impedance is modulated by controlling the flow-rate of hydraulic fluid from one side of a double acting cylinder to the other by means of an electronic servo valve (as conceptually depicted in figure 6). A parallel spring is used to return the ankle to the neutral position after toe-off when the modulated damper is set to a low value during swing flexion.

The simulation model is obtained by combining (3.1) and (3.2) that provide the solution for the total ankle angle as a function of ankle torque and a modulated damping coefficient, (3.3). The total ankle moment, τ_A , is transferred through the parallel damper and return spring that is in series with the spring foot, (3.2).

$$\tau_A = k_f \theta_f = b \dot{\theta}_d + k_r \theta_d \quad (3.2)$$

$$\theta_A = \frac{\tau_A}{k_f} + \int \frac{\tau_A - k_r \theta_d}{b} dt \quad (3.3)$$

3.3 Data Collection

The input of the adaptive ankle prosthesis model is ankle torque. To obtain the real-world input to the system, biomechanics data was collected with unilateral transtibial amputee subjects traversing both a ten degree incline and decline in a single step. A ten degree slope was chosen to represent an extreme that might be encountered in an outdoor setting without placing significant demands on the test subject. Further, it has been shown in able-bodied persons that if the ground slope of the initial step is greater than fifteen degrees, changes gait posture may occur [4]. For this study, all data collected were on level ground or ten degree slopes to avoid changes in gait form.

Two unilateral amputee subjects were recruited through O&P Labs, Springfield MA. Note that all aspects of the study described herein were approved by the University of

Massachusetts-Amherst Institutional Review Board, and all subjects signed informed consent forms prior to the participation. Exclusion criteria included bilateral transtibial amputees, younger than 18 years of age or older than 55 years of age, overweight, physically unfit, confounding medical condition that would place the subject at risk, and a poor sense of balance with a history of falling. Subject #1 was a 34-year-old female (1.78 m, 70 kg) more than 15 years post amputation. Her daily-use prosthesis was an Ossur LP Vari-Flex. Subject #2 was a 42-year-old male (1.88 m, 102 kg) more than 20 years post amputation. His daily-use prosthesis was an Ossur Modular III Category-7. The experiments took place in the Biomechanics Laboratory in the Kinesiology Department at the University of Massachusetts Amherst.

TABLE 1 SUBJECT DESCRIPTION

	Subject 1	Subject 2
Sex	Female	Male
Height	1.78 m	1.88 m
Weight	70 kg	102 kg
Age	34 years	42 years
Prosthesis	Ossur LP Vari-Flex	Ossur Mod III

While walking at their self-selected pace on a level surface, subjects approached either the inclined or declined surface measuring 0.75 m in length. They took a single step with their prosthetic-side landing heel first or foot flat on the sloped surface and then continued on a level surface at the new elevation. The subjects repeated the trial until 10 successful trials for each test were completed for both sound and prosthetic leg. A successful trial was defined as walking at a steady speed and stepping on incline or decline with only the appendage of interest without visibly altering their gait. It should be noted that no difference in the body mechanics is observed

in healthy biomechanics when landing heel first or foot flat on an incline [4]. The biomechanics data were recorded as the subject traversed the sloped surface.

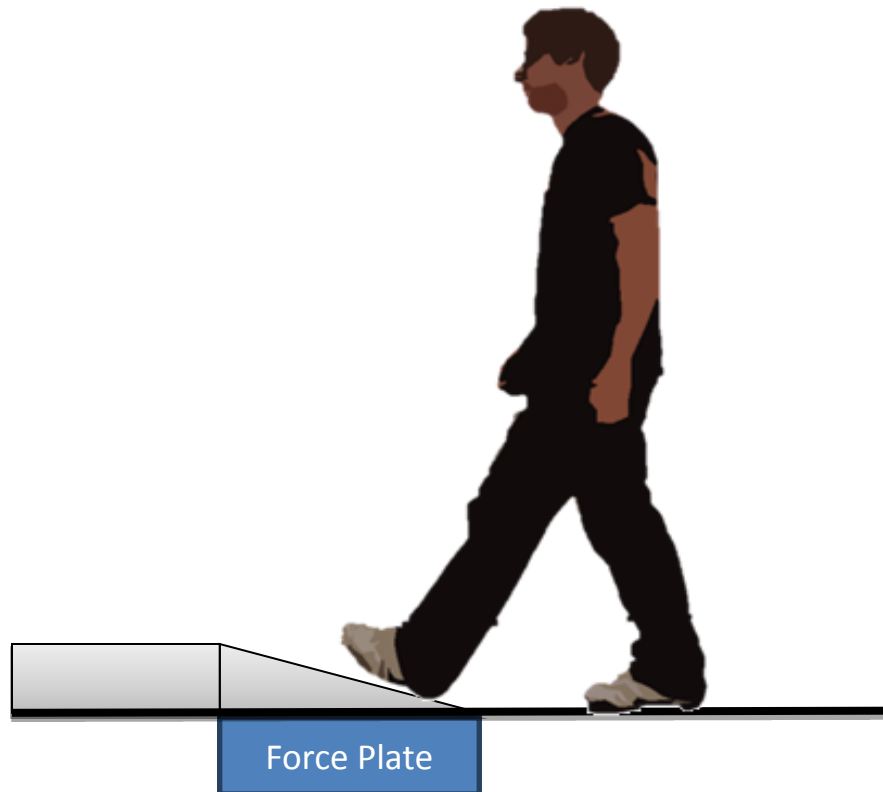


Figure 7. Experimental setup showing subject knowingly stepping onto an altered terrain at a self-selected pace while ground reaction forces and limb trajectories are recorded.

The experiments took place in the Biomechanics Laboratory at the University of Massachusetts, Amherst. The analysis used an eight-camera Qualisys Oqus 3-Series optical motion capture system operated by Qualisys Track Manager software (Qualisys, Inc., Gothenberg, Sweden) to sample test subjects fitted with reflective infrared tracking sensors, at 240Hz. Ground reaction forces were recorded with a floor mounted strain gauge force platform (OR6-5, AMTI, Inc. Watertown, MA, USA), on which the ramps were placed. The force platform recorded the shear forces in two directions and normal forces. The calibration markers

were placed at the following anatomical features to reconstruct the bone structure during data processing: 1st and 5th metatarsals, medial and lateral knee joint as well as ankle malleoli, and the greater trochanters in order to reconstruct points of rotation. Four tracking markers were fixed to each foot, shank, and thigh, as well as the hip segment throughout all testing to track the trajectories of each segment. On the prosthesis, virtual malleoli markers were created during the post-processing of the data by mirroring the able side to represent the prosthesis center of rotation. It should be noted that this assumption for the prosthetic-side can only provide approximations of the actual joint motions and moments. The data were processed using Visual 3D v4 software (C-Motion, Inc, Rockville, MD, USA) to calculate all joint positions, velocities, moments, and power. Table 2 lists the markers and their locations for each segment needed to record each ankle's biomechanics.

TABLE 2 Marker placement

Segment	Calibration	Tracking
Shank	Lateral Knee Medial Knee Lateral Malleolus Medial Malleolus	Shank (4)
Foot	Lateral Malleolus Medial Malleolus Metatarsal 1 Metatarsal 5	Toe (1) Heel (3)

Once all markers are attached, a calibration file is created. This is done by first zeroing the force plate, calibrating the cameras, and then recording the subject standing still facing in the walking direction with their feet shoulder width apart for at least ten seconds. Each series of experiments needs its own calibration file unique to the subject, as well as the day recorded.

From this calibration file, an AIM model can be created, which the QTM software uses to name each marker automatically when applied to movement files. Once this is done, the calibration markers that are placed on the joints can be removed, since their locations can be calculated by the positions of the tracking markers. The experiment can now be recorded into movement files.

When recording each experiment trial, the recording always was started and stopped five seconds before and after the gait cycle of interest to ensure all data was captured. The subject was to start walking at least ten feet before stepping on the platform, and to continue to walk for at least ten feet afterward in order to ensure that the stride was natural to them. After the cycle was recorded, the data was truncated to 10 frames before and after the cycle of interest. At this time the data was inspected to make sure that all tracking markers were recognized. Many times the AIM model fails, and markers must be renamed manually. This proved to be a tedious process and can take a long time. Also at this time, the trajectories of the markers must be inspected to ensure that there aren't any gaps in the trajectories where sufficient data wasn't recorded about the markers. Most times gaps can be filled by interpolating over them. However if a segment doesn't have at least three tracking markers shown at all times that trial must be thrown out.

At this time, all movement files and calibration file exported in c3d format so that it can be processed further in Visual 3D. Uploading the calibration file, a model of the subject's legs is created defining each segment. At this point, a "virtual ankle and foot" were created on the prosthesis side by mirroring the placement of the malleoli tracking markers from the intact foot. This method results in relative values for ankle angles and torques based on where the malleoli should be anatomically located. Oftentimes prosthetic feet have bumps where the malleoli

should be, however these are just for aesthetics and don't reflect the correct position of the joint on the individual being tested. Figure 8 shows a completed model built using a calibration file.

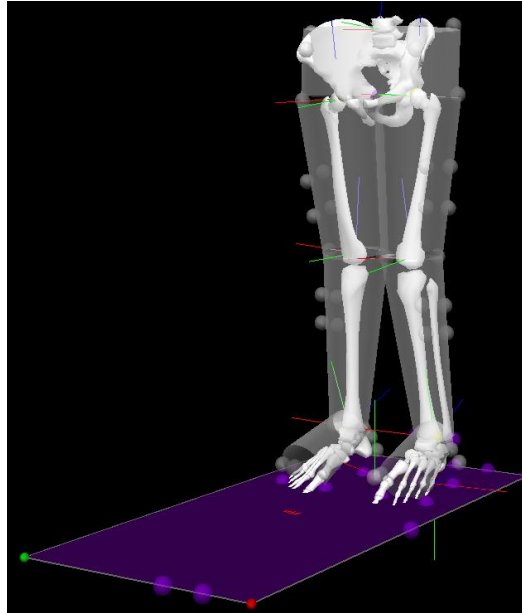


Figure 8. Model created from a standing calibration file, used to calculate biomechanics data from movement files with calibration and tracking markers shown.

Once the model is created, the ankle angle, velocity, torque, and power were calculated for each trial, and averaged together for each specific experiment. A 2nd order butterworth filter with a cutoff frequency of 50 Hz was used to filter out ambient noise before calculations. At this point, a graphical representation of the results can be attained; however the torques and angles were needed for inputs and comparisons for the simulation, so the data were exported to a MATLAB file.

3.4 Methodology

Using MATLAB Simulink, (3.3) was modeled. The prosthetic-side ankle torques for each test subject were entered as the system input. In this approach, the power loss of the modulated damper is ignored. The effect of this assumption is that more energy will be stored in the foot spring that would be returned during push-off. Since this simulation focuses on the kinematic response, the simulation remains valid for studying the effects of adding a damper in series with a spring foot.

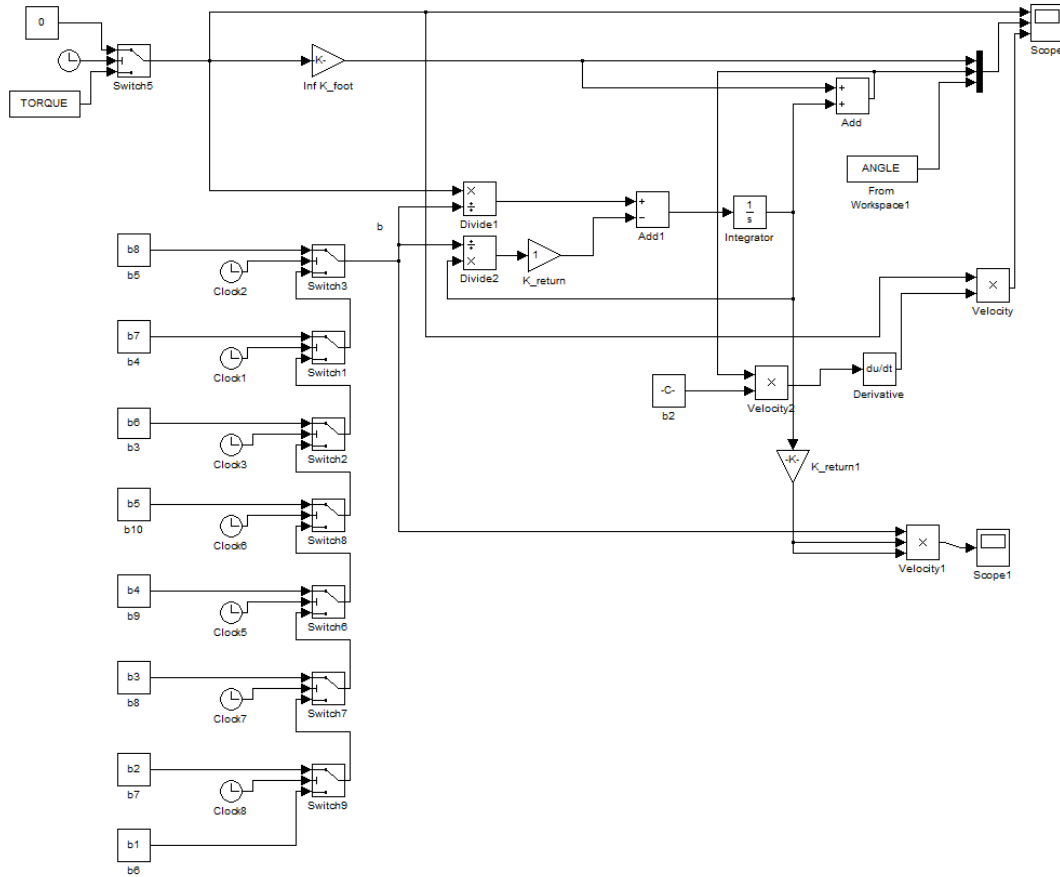


Figure 9. MATLAB Simulink model used to simulate the addition of a damper in series with the carbon spring foot from the biomechanics data recorded.

To tune the damping coefficient b , eight recognizable events were chosen. The events chosen were chosen since they are easily recognizable in any person's gait cycle. The damping constant for each phase was tuned manually to closely mimic the healthy biomechanics during slope walking [22]. For example, at heel strike the initial damping value is set very low to allow the ankle to adapt to the ground slope. The second event occurs just after heel strike and increases impedance of the system to provide support and prevent toe-slap. Subsequent events occur at inflection points in the torque profile (where the ankle acceleration would be zero). Through an iterative tuning approach, it was found that altering the damping at these points allows for smooth simulated angular accelerations. The events are shown graphically in figure 10. The stiffness of the foot spring was found by independently linearly fitting angle-torque response during controlled plantarflexion and controlled dorsiflexion to model the heel and toe stiffness, respectively. The stiffness of the return spring (1.0 N-m/deg) was chosen to provide the appropriate response during swing to provide toe clearance.

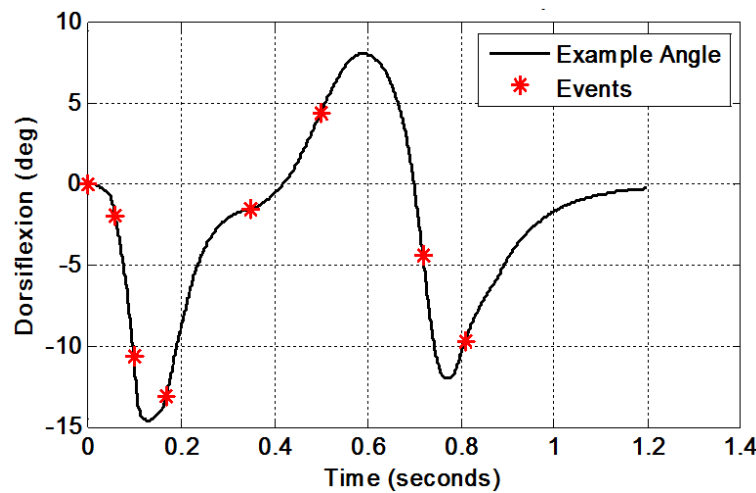


Figure 10. Identifiable gait events that mark the changes in the damping coefficient shown on an example adaptive ankle angle plot.

3.5 Results and Discussion

Figure 11 presents a kinematic comparison of the amputee wedge stepping study and the adaptive ankle prosthesis simulation to able-bodied sloped walking data. The tuned damping coefficients corresponding to each gait event from figure. 10 are presented in Table 3. Using the biomechanics data, the stiffness of the foot and heel of the subjects' daily-use prostheses were found to be 2.9 and 12 N-m/deg for Subject #1 and 3.7 and 10 N-m/deg for Subject #2.

TABLE 3 Damping coefficient (N-m-s/deg) updates at different events

Event	Subject 1			Subject 2		
	Level	Up	Down	Level	Up	Down
1	0.1	0.1	0.1	0.1	0.1	0.1
2	0.12	0.12	0.4	0.15	0.2	0.1
3	0.5	0.8	0.8	0.5	0.8	0.2
4	1000	1000	1000	1000	1000	1000
5	1000	1000	3.0	1000	1000	8.0
6	100	100	2.0	100	100	4.0
7	0.5	10	1.0	1.0	10	1.0
8	0.1	0.1	0.1	0.1	0.1	0.1

-For each simulation, the damping coefficient b is updated once immediately following heel strike before foot flat, and at the inflection points of the input torque.

-A damping coefficient of 1000 simulates a very high stiffness that would occur if the damper were locked by closing the valve completely. Practically, the damping coefficient would be limited by the leakage across the cylinder and valve seals.

In comparing the kinematic data of each transtibial amputee's passive prosthesis to able-bodied data, it is evident that key adaption characteristics are missing. Specifically, after heel strike during controlled plantarflexion response proportional to the ground slope is observed in the able-bodied and adaptive prosthesis, but not in the passive prosthesis. The able-bodied data of the ankle angle increases throughout controlled dorsiflexion to a maximum ankle angle.

Through the plantarflexive torque the adaptive prosthesis is able to leverage the summation of foot spring and damper to closely match the able-bodied data. During this same phase, the spring foot only exhibits nearly the same behavior on each slope. Lastly, the adaptive foot/ankle prosthesis returns to the neutral position after toe-off, by means of the return spring in parallel with the modulated damper. This characteristic is not required in the passive spring foot because its neutral position does not vary.

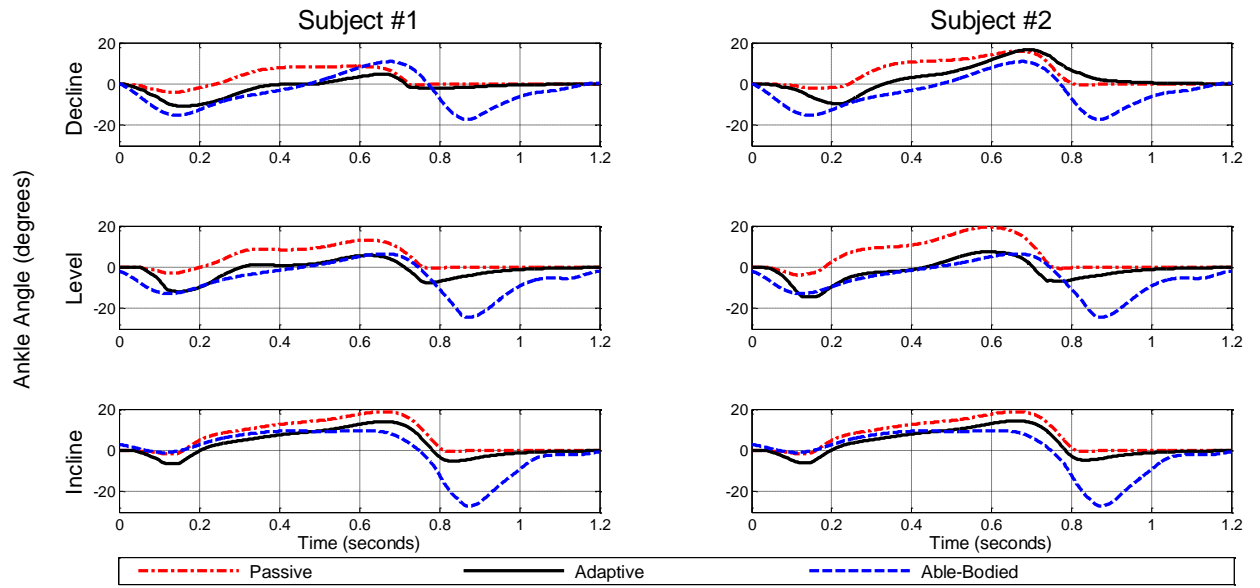


Figure 11. Adaptive ankle simulation compared with the subject's passive spring foot/ankle and able bodied data[22]on level ground and ten-degree inclines and declines.

In reviewing the tuned damping coefficients in Table 3, a ramp-type function is observed. The initial damping coefficient is low to allow for ground slope adaptation, but preventing the toe from slapping the ground. After initial adaptation, the damping coefficient increases to effectively lock the position towards the end of controlled dorsiflexion. Just before toe-off, the coefficient decreases to allow for increased dorsiflexion (comparable to able-bodied data). On declines, the coefficient decreases earlier in order to allow for increased dorsiflexion, accommodating the slope.

It is important to note that the overall stiffness of the semi-active ankle prosthesis cannot be larger than the stiffness of the carbon fiber foot. If the ankle angle is greater than that of the desired trajectory of a given slope, the angle could not be corrected. For this reason, it was found that the effective ankle stiffness could be lowered via a low damping coefficient on heel strike, to identify the ground slope and correctly modify the gait profile during the rest of the stance phase. In this manner, it is shown that the simulated ankle angle better represents the ankle angle of an able-bodied individual than a passive prosthesis with no damping.

Implementing this approach would leverage a supervisory controller to monitor activities and terrain conditions. The position/velocity/torque response of the impedance-based ankle prosthesis would encode whether the user is walking on level, declined, or inclined surface. A state controller could then be used to switch the damping coefficients based on the identifiable gait events. These controllers would use on-board sensors that monitor the position and pressure of the hydraulic chamber (ankle torque and position) as well inertial measurements. This study presents a starting point for the development of an intelligent passive prosthesis that has the ability to modulate its internal damping characteristics to conform to the ground slope at each step.

CHAPTER 4

A SEMI-ACTIVE DAMPING DESIGN FOR USE IN A TERRAIN ADAPTIVE ANKLE PROSTHESIS

Adapted from a Technical Paper published in the *Proceedings of the 2011 International Mechanical Engineering Congress and Exposition* [2]

Abstract— State-of-the-art commercial ankle prostheses enable amputees to walk on level ground replicating the passive biomechanics of able-bodied persons reasonably well. However, when navigating uneven terrains (such as slopes and stairs) these devices do not allow the ankle to adjust to the ground at each step in order to maintain stable contact. At these instances, the probability of falling is greatly increased. In contrast, the natural ankle adapts passively (i.e. no net positive power is required) just after heel strike allowing the foot to conform to the ground. This paper focuses on developing a continuously variable damper that can be paired with a carbon fiber foot in order to replicate the passive adaption dynamics of the human ankle. Presented in this paper are the performance specifications, the mathematical model, and the resulting device design for the semi-active damping system. The design consists of a hydraulic actuator, coupled to a servo control valve which modulates the damping. The system is designed to replicate the dynamic damping range of an able-bodied ankle joint by achieving flow rates as high as 2.0 liters per minute at 1.0 MPa, and operate at up to 20 MPa.

4.1 Introduction

The incidence of lower limb amputation in the United States as of 2005 is one out of every five hundred persons with over 600,000 persons living with major lower limb [23]. Factoring the prevalence of dysvascular diseases such as diabetes, as well as the general aging of

[3]the US population, the number of amputees living in the United States is expected to double by the year 2050 [24].

Passive prostheses commercially available to lower limb amputees today have been optimized for level ground walking. State-of-the-art foot/ankles are carbon fiber springs that cannot adapt on a step-by-step basis to varying terrains (such as walking on slopes, descending and ascending stairs, and while standing up from a seated position). The inability of the ankle prosthesis to adjust creates potentially unsafe conditions for amputees, especially if there is a sudden unexpected disturbance such as stepping on a rock or curb. Studies have shown that the falling incidence rate in the amputee population exceeds that of the institutionalized elderly [25], and about one out of ten lower limb amputees have reported requiring medical attention for a fall that has occurred within the year. A factor that can be attributed to the increased rate of falling is the inability of the prostheses to provide stable ground contact on all terrains [26]. To address this deficit, a semi-passive, intelligent ankle prosthesis for lower limb amputees is being developed.

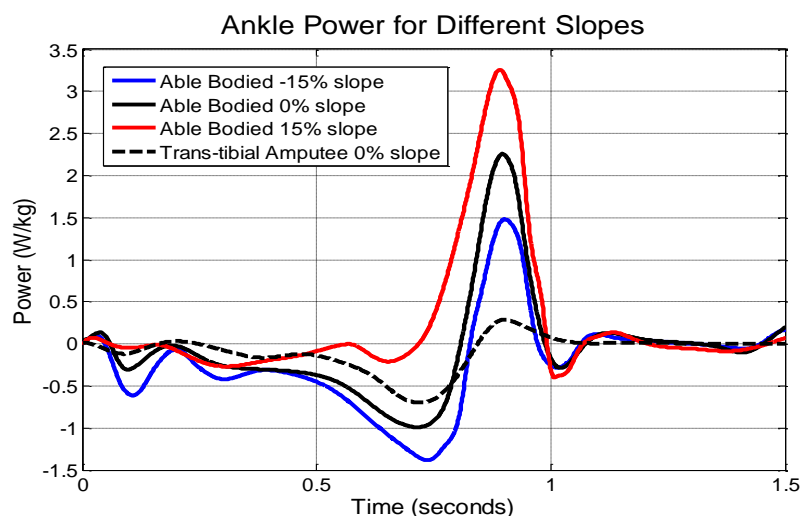


Figure12. Ankle power of able-bodied and transtibial amputee during self-selected speed walking showing 0%, +15%, and -15% slope data for able bodied persons [7], and 0% slope for transtibial amputees using passive prostheses [8].

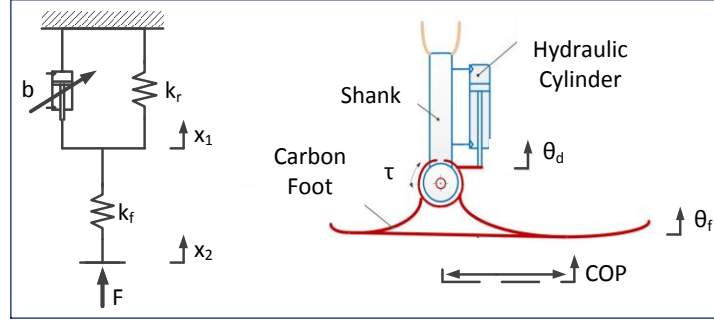


Figure13. Spring-damper model representing a carbon-fiber foot with stiffness k_f , in series with a modulated damper with variable damping coefficient b , and return spring with stiffness k_r in the linear domain (left) and rotational domain (right). In the linear domain, damper displacement is noted as x_1 , and foot flexion is denoted as x_2 . In the rotational domain, they are denoted as θ_d and θ_f .

Due to eccentric activity of the muscles, the net ankle power during the first half of the normal walking gait cycle is dissipative for able-bodied persons which can be seen in figure 12. It is during this phase of gait that the healthy ankle adapts its behavior to provide stable ground contact in order to bear weight. Since power is not being generated by the ankle during this phase, the ankle's behavior can be replicated with passive elements, (i.e. a spring and damper). To accurately mimic these trajectories, the system needs to be able to modify its dynamics in real-time. In order to accomplish this, a variable hydraulic damper (i.e. semi-active damping) is placed in series with the spring foot. The power that is being dissipated during the adaptation phase is used to modulate the overall behavior of the ankle. A return spring is used to restore the neutral equilibrium position during swing. The system configuration of the prosthetic ankle design can be seen in figure13. The ankle's behavior is effectively modulated by controlling the flow-rate of hydraulic fluid from one side of a double-acting hydraulic cylinder to the other.

In this paper the authors' describe their progress on the development of an ankle prosthesis that leverages semi-active damping to continuously adapt to changes in the terrain. This paper describes the prior works in the terrain adaptive ankle prostheses, the enabling

biomechanics that justify a semi-active damping approach, the development and optimization of compact variable damper and a test bed for its characterization, and concludes with simulation results and a discussion on the future direction of the work.

4.2 Prior Works

Conceptualized in the 1950s, the Mauch Ankle is the first documented effort on the development of a slope adapting ankle prosthesis. The passive hydraulic ankle prosthesis provided damping while walking to prevent toe-slap at heel strike and adapted to the ground slope through a hydraulic mechanism that locked the ankle at mid-stance for support. A spring returned the foot to a neutral position after toe-off. The device was well received by amputees, but mechanical failures and hydraulic leaks prevented the device from being commercialized [17], [27]. Inspired by the Mauch Ankle, a foot/ankle developed at Northwestern University provides ground slope adaption that uses static friction (as opposed to hydraulics) to lock the ankle after it has conformed to the ground slope. The device does not provide damping, and in its current state has a limited mechanical lifespan due to wear [28].

A commercial foot/ankle Echelon is a passive prosthesis that provides manually set hydraulic damping for both plantar and dorsiflexion, and the ankle is returned to the neutral position after toe-off by a return spring. Similarly, another commercial device, Motionfoot by Motion Control, is a hydraulic foot/ankle damper that can be manually adjusted to reduce toe-slap at heel strike. For support during gait, a non-adjustable hard stop prevents the ankle from moving past the neutral position. This design adjusts the ankle (without locking it) while walking down slopes, but cannot adjust on ascents due to the fixed hard stop. This device does not include a spring to return the ankle to neutral position after toe-off.

The only electromechanical terrain adapting device is the Proprio Foot by Ossur. It adapts to sloped surfaces over multiple strides through onboard inertial sensors that estimate the ground slope of the current step and adjust the ankle's position during the swing phase. Continuous step-by-step adaption is prohibited by its low-power design that is not able to adjust the ankle angle while bearing weight. Further, its control algorithm assumes the ground slope of the next step will be the same as the current step (i.e. there is a learning period and would not protect against sudden slope changes such as stepping on a curb). None of the above described devices offer intelligent dynamic adaptation to the terrain. The lack of adaption can regularly create periods of instability during daily use that could potentially result in a fall.

4.3 Damper Design

From able-bodied and unilateral transtibial amputee biomechanics [7], [8], performance characteristics of the ankle prosthesis were identified. Design limitations such as maximum allowable working pressure and material properties were also evaluated in order to constrain the optimum design configuration. Table 4 shows the design parameters, constraints, and performance criteria. The objectives are to design an ankle that has the capability of replicating the human biomechanics during the adaptation phase, and is as light as possible.

It is shown that a normal walking strategy is used for traversing wedges up to 15° [4]. For this reason, the ankle angle operational envelope θ_{\max} for the initial design will be limited to $\pm 15^\circ$, allowing the ankle to be displaced a maximum of $\pm 15^\circ$ even if there is no flexion in the spring foot.

The maximum ankle moment that the damping system needs to be able to develop was derived from the peak ankle moment observed during normal walking of transtibial amputees when walking with passive spring/foot prostheses. Greater moments are observed in able-bodied

persons due to their ability to push off with positive power. Since the passive prosthesis does not have this capability, amputee biomechanics were used. The ankle needs to be able to support 1.2 N-m/kg during the stance phase [8], or 120 N-m for a 100 kg person which is denoted as M_{max} .

Valve and hydraulic line specifications are developed from the maximum angular velocity and peak pressure profiles from the requisite moments. The maximum angular velocity of a passive prosthesis reflects the rate that the carbon foot is able to flex. However, to enable adaption the semi-active damping prosthesis requires a higher peak velocity. For this reason, the maximum angular velocity that the adaptive ankle prosthesis needs to replicate is dictated by the maximum angular velocity seen in healthy biomechanics during the first half of the gait cycle. It is important to note that the human ankle response is passive during this portion of the gait cycle. This was observed to be 150 degrees per second.

TABLE 4 Design parameters constraints and performance criteria

Design Parameters		
x(1)	Cylinder Inner Radius	>12.7 mm
x(2)	Damper Moment Arm	<50.0 mm
x(3)	Cylinder Outer Radius	<15.8 mm
Design Constraints		
P_{max}	Maximum Allowable Pressure	20 MPa
σ_{max}	Maximum Allowable Stress	225 MPa
Performance Criteria		
M_{max}	Maximum Ankle Moment	120 N-m
θ_{max}	Angle Operational Envelope	$\pm 15^\circ$
$\dot{\theta}_{max}$	Maximum Angular Velocity	150°/s

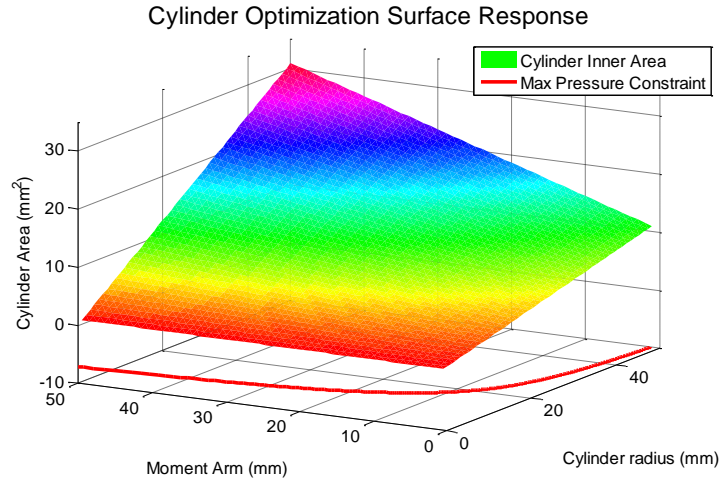


Figure 14. Cylinder optimization surface response with inner radius and moment arm as design parameters shown with the maximum allowable working pressure nonlinear constraint.

To accomplish this, a double-acting double rod-end differential damper is being designed. A standard single rod-end was not chosen in order to eliminate the need for an accumulator, which stores excess hydraulic fluid in systems that have different volumes at different operating points. A double rod-end differential damper has a constant containment volume at all operating points. The damper consists of a steel cylinder with two aluminum end caps, and houses an aluminum piston a rod on either side, each with a return spring.

$$f(x) = 2 * pi * x(1) * (l_{piston} + 2 * x(2) * \sin(\theta_{max})) \quad (4.1)$$

An optimization was performed on the cylinder since it dictates the size (and mass) of all the mating components. In order to minimize the weight of the cylinder, an objective function was written shown in Equation 4.1.

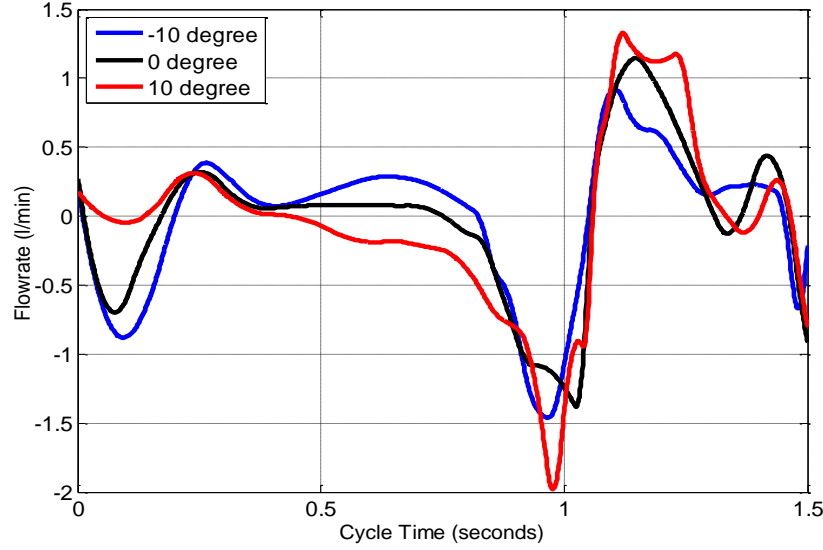


Figure 15. Simulated damper flow rates for the adaptive ankle prosthesis during level and sloped walking.

This equation represents the interior surface area of the cylinder as a function of the inner radius $x(1)$, and the moment arm $x(2)$ that the damper acts on the ankle joint. The cylinder material volume was not considered immediately since the wall thickness needed varies little with the inner radius. The length of the piston l_{piston} is constrained by the seal design specifications (Trelleborg Sealing Solutions). θ_{max} is the maximum angle away from the neutral position that the ankle will need to be displaced to during normal walking, which is 15 degrees. Before analyzing the optimization problem, the minimum rod diameter r_{rod} was calculated to be 5 mm using Euler buckling theory with a safety factor of 2.

The primary constraint of the design is the maximum allowable pressure P_{max} of 40 MPa which is defined by the design specifications of the seals (Trelleborg Sealing Solutions). For a design safety factor of 2, P_{max} was set to 20 MPa. This nonlinear constraint which can be seen in Equation 4.2 is also written as a function of the inner radius $x(1)$ and moment arm $x(2)$. As long

as parameters lay on this constraint, the flow rate through the valve is also minimized allowing for a smaller valve and hydraulic lines.

$$P_{\max} \geq M_{\max} / \left[x(2) \left(\pi(x(1)^2 - r_{rod}^2) \right) \right] \quad (4.2)$$

The nonlinear optimization problem was solved using MATLAB. The surface response can be seen in figure 14, with the nonlinear maximum pressure constraint shown as the red line. The problem solved to have the least inner area with an inner radius of 7 mm, and moment arm of 65 mm. This turned out to be an unrealistic design since fabrication of such a small diameter damper would be difficult, and had to be bounded by the dimensions of materials that are available. The smallest honed cylinder that was found has an inner radius of 12.7 mm. This value was set as the lower bound for $x(1)$. To optimize the wall thickness, the objective function was rewritten as the volume of the cylinder, where $x(2)$ is still the moment arm, and the outer radius is a new design parameter $x(3)$. This is seen in Equation 4.3.

$$f(x) = \pi \left(x(3)^2 - r_i^2 \right) * \left(l_{piston} + 2 * x(2) * \sin \theta_{operation} \right) \rho_{steel} \quad (4.3)$$

The optimization was then constrained by the maximum allowable hoop stress σ_{max} . The material properties of the tubing were not given by the manufacturer, so it was assumed have the properties of standard structural steel. This constraint can be seen in Equation 4.4.

$$\sigma_{\max} \geq \left[\left(P_{\max} r_i^2 - P_a x(3)^2 \right) / \left(x(3)^2 - r_i^2 \right) \right] - \left[r_i^2 x(3)^2 (P_a - P_{\max}) / r_i^2 \left(x(3)^2 - r_i^2 \right) \right] \quad (4.4)$$

Equation 5.3 solves for the minimum outer radius needed to be a minimum of 13.88 mm. The moment arm corresponding to the maximum allowable pressure constraint was calculated to be 23.3 mm. The cylinder wall thickness was verified using the shape optimization tool in

ANSYS WB, which came within 1% of the calculated thickness. The difference can be attributed to the algorithm used to calculate stress used in the ANSYS program.

The piston length and profile were designed to accept two wear rings, and one seal ring as specified by Trelleborg Sealing Solution. The piston will be fabricated out of lightweight high strength aluminum allow AA-2024. The end caps were also designed according to the specifications given by Trelleborg Sealing Solutions to each house one wear ring, one seal ring, and one wiper to ensure that there would be minimum leakage, and that the seals could be installed properly without damage. The material to be used is also AA-2024 high strength aluminum alloy. The caps will be attached to the cylinder with M30 X 1.5 threads, and the threads will be sealed with high pressure anaerobic thread sealant.

In order to specify the hydraulic line size needed, a simulation was performed modeling the ankle as seen in figure 13 with Equations 4.5-4.7, and calculating the flowrate as a function of damper speed $\dot{\theta}_d$ using prosthetic side ankle torque τ_A data and prosthesis foot flexion from collected in a previous sloped walking study as inputs (LaPrè 2011). The simulated damper flow rates are shown in figure 15.

$$\theta_A = \theta_f + \theta_d \quad (4.5)$$

$$\tau_A = k_f \theta_f = b \dot{\theta}_d + k_r \theta_d \quad (4.6)$$

$$\theta_A = \frac{\tau_A}{k_f} + \int \frac{\tau_A - k_r \theta_d}{b} \quad (4.7)$$

Using industry standards for sizing hydraulic lines, it was determined that 6.3 mm (1/4 inch) ID tubing would be sufficient for the design of this hydraulic damper. In order to specify a servo valve, performance specifications were also dictated by the maximum flow rate needed, as

well as the maximum operating pressure of 20 MPa. The valve chosen is E024 weighing 92g which operates up to 21 MPa, and has a maximum flow rating of up to 7.0 l/min at 7.0 MPa pressure drop.

The final calculated weight of the damper is just over 300g. The assembled design and exploded view can be seen in figure 16 highlighting the major components. Return springs have been added to the design to enable the damper to return to the zero position during swing. The return spring constant k_r was varied during damper simulations in MATLAB, and a constant of 1.0 N-m/deg, or 35 N/m in the linear domain. This however is subject to change once the damping system is characterized in future physical experiments once the damper is fabricated. A trunnion mount clamped around the cylinder is used to attach the damper to the ankle structure, and a clevis mount rod end is used to attach to the moment arm. All pivots have been designed with commonly available bushing type bearings.

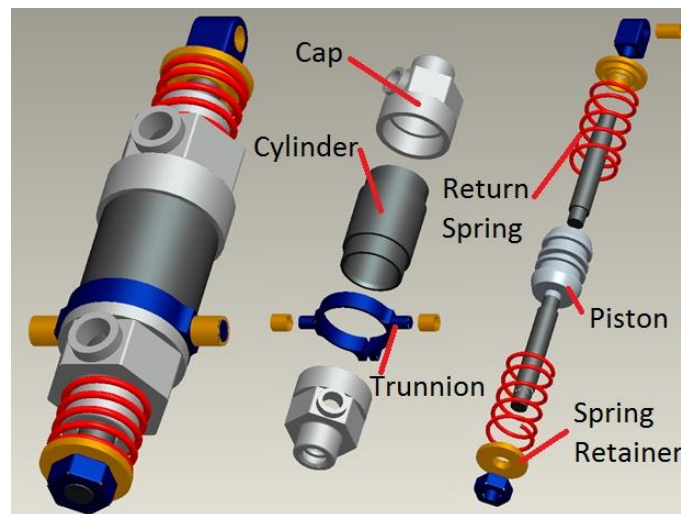


Figure16.Damper assembly (left) and exploded view (right).

The damper will be mounted in an ankle test apparatus shown in figure 17. The structure will allow the damper to pivot about the trunnion clamp, and apply a torque to the ankle joint through the moment arm. An Ossur LP Vari-Flex will also be mounted rigidly to the moment arm so that it acts in series with the damper about the joint.

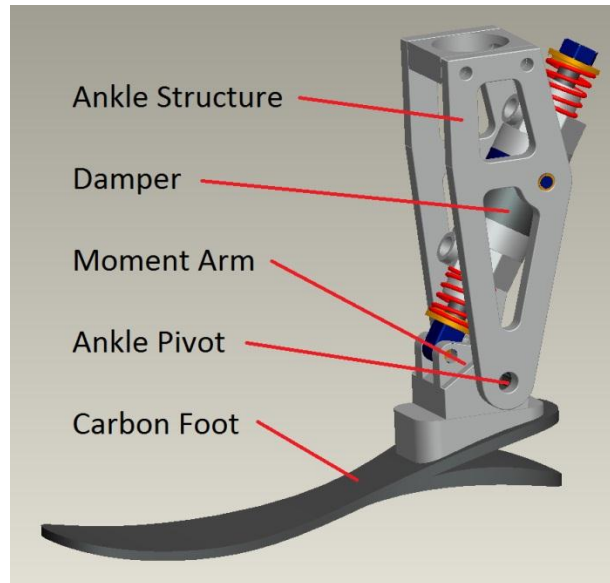


Figure 17. Damper shown installed in an adaptive ankle prosthesis prototype.

4.4 Test Bed Design

In order to characterize the damping system, a test bed has been designed to act as a driving dynamometer, figure18. The apparatus will also be used extensively in the development of control algorithms in the future. The performance requirements of the test bench are calculated by transferring the ankle performance requirements to the linear domain. It needs to drive the damper at a maximum of 60 mm/s, and provide a maximum of 5.4 kN at stall to simulate a 100 kg person.

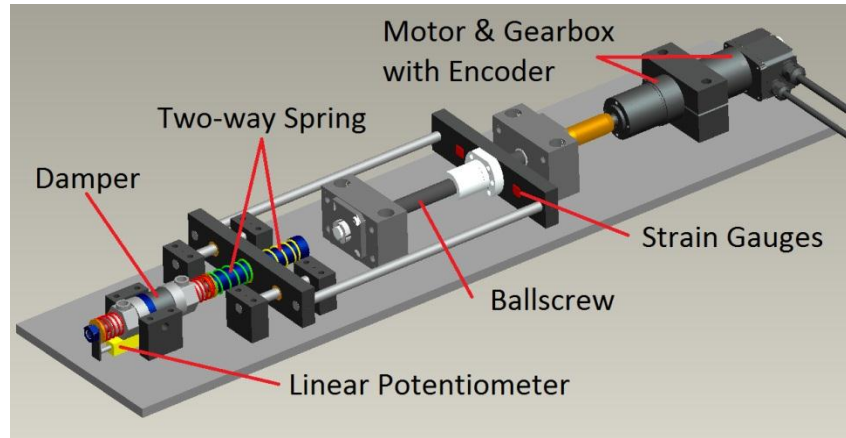


Figure 18. Damper test bench shown with key components labeled.

To reduce the complexity, an electromechanical system was designed, consisting of a motor, gear head, and ball screw, to drive the damper. A brushless DC motor (Maxon EC-45, 136212) coupled to a planetary gearbox (Maxon 203114) with gear ratio of 4.3:1 meeting the specifications was selected to turn a 16 mm diameter Nook ball screw with a 2 mm lead in order to meet the desired performance specifications. The ball screw drives a two-way independent spring set up that simulates the carbon foot heel stiffness in one direction past the equilibrium point, and the carbon foot toe stiffness in the other opposite direction. Based on experimental data and the moment arm to be used in the new ankle prosthesis, the heel stiffness k_h is calculated to be 1,380 N/mm, and the foot toe stiffness k_f is calculated to be 334 N/mm. Strain gauges are mounted between the ball screw and spring assembly to act as a load cell. The Maxon motor is fitted with a programmable rotary encoder (CUI AMT-102) to track input displacement, and the damper is equipped with a linear potentiometer in order to track the damper displacement.

4.5 Simulated Results

As part of a prior work (LaPrè 2011), a wedge stepping study was performed in a biomechanics motion capture lab. Amputees were tasked to walk at a self-selected speed and then stepping knowingly onto inclined and declined wedges that were placed on a force platform. The studies described herein were approved by the University of Massachusetts-Amherst Institutional Review Board, and all subjects signed informed consent forms prior to participation in the study. This data was used to simulate the addition of a damper in series with the carbon fiber foot used, and compared to able-bodied data. Biomechanics data example in figure 19 were collected with a unilateral transtibial amputee subject 15 years post amputation wearing her daily-use passive prostheses while traversing both a ten-degree incline and decline in a single step (Subject Info: 34-year-old female, 1.78 m, 70 kg, prosthesis: Ossur LP Vari-Flex).

The adaptive ankle prosthesis was modeled as shown in Equations 5.5-5.7, and the torque calculated from the amputee wedge data was used as the torque input (τ_A) and the ankle angle (θ_A) is the output. Figure 8 shows the simulation of the adaptive ankle prosthesis' reaction when an amputee steps on a ten-degree decline from a level surface. By altering the damping coefficient at each ankle angle inflection point, the resulting ankle angle response better resembles that of an able-bodied person (LaPrè 2011). For terrain adaptation, this is especially important during controlled plantar flexion when the ankle is conforming to the ground slope. A supervisory controller will be able to modulate the damping coefficient continuously based on sensor measurements such as ankle angle and velocity, ground reaction forces, or inertial measurements of the foot and shank. In this manner the ankle trajectory of the adaptive prosthesis will better resemble that of able-bodied persons during controlled plantar flexion and controlled dorsiflexion phases of gait.

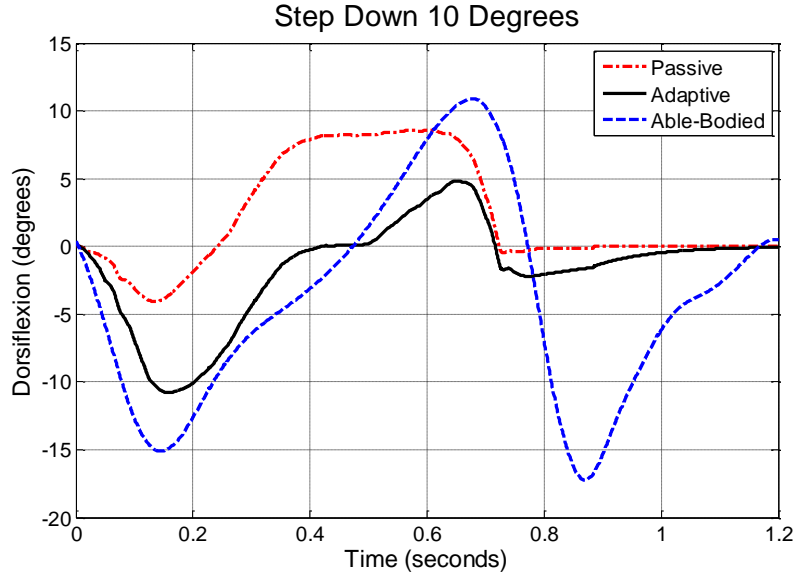


Figure 19. Simulation of the adaptive ankle which takes inputs of existing amputee prosthesis ankle torque data and outputs the simulated ankle angle, compared with the passive ankle prosthesis data and able-bodied data [7], for stepping on a ten-degree decline from a level surface.

4.6 Post Publication Design Changes

The damper has been fabricated with minor changes to the design. The piston was shortened by removing the chamfers that were previously incorporated for seal installation. It was decided that the extra material was not needed since a tapered sleeve could be made to slide over the piston, allowing the seal to be stretched safely for installation. This allowed the steel cylinder to be shortened considerably. The end caps needed more material to safely drill and tap the hydraulic line connection ports since it was determined that bosses for the ports could not be safely welded to the caps without warping. Even though the weight of the caps increased, the changes brought the total weight to 250.7 g which is 16.4% less than the original design.

Due to the timeline, the entire test bed design was revamped with an integrated actuator assembly from Exlar Inc. in order to eliminate the complexity of having to couple a motor to a

ball screw. A Pololu 12V geared motor with encoder was attached to the manual valve to act as a servo to enable computer control of the damping. In order to represent the carbon spring foot physically in the linear domain, a spring mechanism had to be designed that had independent stiffness values for both positive and negative deflection displacements. This represents the separate stiffness values of the heel and toe in a carbon spring foot during plantar flexion and dorsiflexion. More technical specifications of the test bed can be found in chapter 5.

CHAPTER 5

CHARACTERIZATION/TESTING OF THE SEMI-ACTIVE DAMPING SYSTEM

Abstract—Today’s passive prosthetic foot/ankles offer little to help the user navigate constantly changing terrains in a safe manner. Fully powered prosthetic foot/ankles require large bulky battery packs that have limited spans. There is a need for intelligent robotic prosthetics that are energy efficient and can make traversing changing terrains not only safer, but less demanding on the user. One option for a foot/ankle prosthesis that has yet to be fully explored or developed is a semi-active system that has the ability to change its passive dynamics continuously based on cues from the user and the environment, with a small energy source, to provide a more stable platform for the user’s weight to be transferred to the ground. This paper describes the characterization and testing of a semi-active damping system developed for use in an intelligent terrain adaptive ankle prosthesis. The damping system is tested in a linear test-bed recording the response to a force input recorded in previous work. The results are then compared to the theoretical performance of the device, as well as able bodied and unilateral transtibial amputee biomechanics data. The results prove the ability of a semi-active damping prosthesis to have more natural biomechanics than ordinary passive prosthetics, with the potential to be operated with small battery sources for long periods of time.

5.1 Introduction

Recent technological advances in computation, actuators, and battery technology has brought about a new generation of intelligent lower limb prostheses. At the knee joint, commercial microprocessor controlled prosthesis such as the Otto Bock C-Leg™, Ossur Rheo Knee™, Freedom Innovations Plié™ and the Endolite Orion™ have demonstrated the benefits

of energy efficient modulation of the knee joint to increase stability [29], [30]. However, modern ankle prostheses replace the ankle and foot with a fixed carbon fiber spring which is optimized for level ground walking [12]. The only microprocessor controlled ankle, the Ossur Proprio™, can only change the ankle position during swing based on estimations prior step. These passive devices cannot adapt to variations in terrain or to the user's activity in a natural or compliant manner. The fixed relationship between ankle flexion and moment, the stiff ankle can produce potentially unsafe conditions for amputees. This is especially true if there is a sudden or unexpected disturbance such as stepping on a rock or curb [13], [15], [31]. This is evident in the falling incident rate in the amputee population, which is equal to that of the institutionalized elderly, and about one out of ten lower limb amputees have reported requiring medical attention for a fall that has occurred within the year [16]. The significant limitation that the range of motion in a passive foot/ankle is directly coupled to the ankle moment through the spring foot severely obstructs an amputee's capability to sustain stable ground contact on terrains that are not level. Consequently there is a significant decrease in the walking stability of an amputee compared to an able-bodied person while walking on slopes [13]. To improve the walking stability of the lower limb amputee, the prosthetic ankle would need to adapt to the terrain continuously throughout every step taken.

The first step response to a new ground slope was studied during the initial step onto an inclined surface with able bodied people (called "wedge stepping") [4]. The biomechanics of the lower limbs and postural changes during the adaptation phase of gait were examined during this study. A similar study was conducted that focused on steady-state inclined walking of lower limb amputees [31]. The study clearly shows that an amputee's hip, knee, and sound ankle trajectories significantly compensate for both the kinematic and kinetic limitations of the ankle when

walking up and down slopes [31]. Since there were no wedge stepping studies found in the literature for amputees, one was performed as part of our prior research. Using the recorded amputee wedge stepping data as an input to a simulation, it was found that incorporating semi-active damping by adding a variable damper in series to the passive carbon fiber spring foot, the amputees' biomechanics would better represent healthy biomechanics in suddenly altered terrains, which is evidence that it will also improve the amputees walking stability [1]. The adaptive ankle concept with a damper in series with the spring foot can be seen in figure. 20.

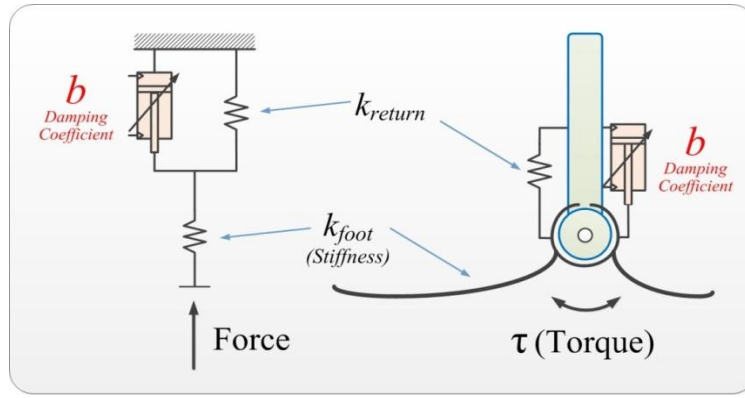


Figure 20. Adaptive ankle concept shown in linear domain (left) and rotational domain (right) consisting of a spring foot with stiffness k_{foot} in series with variable damper b and return spring with stiffness k_{return} in parallel.

In order to implement semi-active damping into an ankle-foot prosthesis, hardware had to be developed since commercially available components which met the strength and weight requirements weren't available. As part of a prior work a dual-acting dual-ended hydraulic damper cylinder was designed minimizing its inner cylinder diameter and moment arm at which it acts on the revolute joint in an ankle prosthesis [2]. The damping impedance is modulated by throttling the fluid flow from one side of the cylinder to the other with a HAM-LET integral bonnet needle valve with a regulating stem tip, and a Pololu geared motor with encoder feedback

for position control of the valve. The geared motor has an output no-load speed of 350 RPM and stall torque of 110 oz-in. The first generation prototype built for the use of control algorithm development via the use of a test-bed can be seen in figure. 21.



Figure 21. First generation fabricated damper and servo-valve used for control development.

In this paper, the authors present their progress with the semi-active damping technology being developed for the use in lower limb prostheses. The damping system testing methodology, characterization, damping control, and testing results found via a custom built test-bed compared to amputee and actual bio-mechanic data for different slopes are illustrated.

5.2 Prior Works

Previous work to incorporate adaptive behaviors into prosthetic ankles began in the 1950s by Hans Mauch [17]. His passive ankle utilized a hydraulic damper to adapt to the ground slope on contact via an event-driven mechanical control valve. After toe-off, a return spring restored the foot to a neutral position. Plagued by mechanical failures, the device was not commercialized, but the device demonstrated the benefits of adaptation. More recently, a friction-based device that adapts to sloped surfaces at heel strike and then locks as the device bears weight was developed at Northwestern University [28]. The Endolite Echelon™ is a commercially available prosthetic foot/ankle is a passive hydraulic prosthesis with independent plantarflexion and dorsiflexion damping values that must be manually set. The prosthesis aims to passively mimic the visco-elastic response of human muscle with fixed damping and spring constants to provide ankle adaptation on sloped surfaces. It is important to note that both the Northwestern and Endolite prosthesis are passive devices and do not have onboard intelligence to modulate their behaviors based on the terrain or the user's activity. The only commercially available at this time with on board intelligence is the Ossur Proprio Foot™. The electromechanical prosthesis uses its onboard sensors and control algorithm to adapt incrementally to slope changes by estimating the ground angle of the current step and then adjusts the ankle during swing. The device assumes the next step will be on the same ground slope. The design of the Ossur Proprio Foot™ can only adjust the ankle angle while it's not bearing weight.

Recent research on fully-active powered prostheses has developed robotic devices with the ability to deliver human-scale torque and power [19-21]. Each of these projects demonstrates the potential to create intelligent prostheses using state-of-the-art technology. Even these fully-

active devices must face the challenge of adapting to changing terrains on a step-by-step basis. The control structure of these devices actively mimics the biomechanical responses of the human ankle through control of active and passive elements. The ability for these devices to enable step-by-step adaption is also complicated by the advantage they offer (i.e. their ability to act in a forceful manner). This requires more detailed knowledge of the terrain and user's activity to coordinate the user and prosthesis in functional interaction during gait. Of the above mentioned prostheses, none modulate the ankle's impedance in real-time based on changes in ground slope to improve the adaptive behavior of the ankle

5.3 Hardware Simulation Test Bed

A custom test bed was designed and built to characterize the hardware and develop control algorithms prior to human subject testing with a prototype prosthesis. The test bed consists of the prototype damper (figure. 21) connected to an electric linear actuator (Exlar T2: M090-0601-GSM) via a 9 kN load cell (Omega: LC202-2K) and custom linear foot spring mechanism. The position of the damper is recorded with a linear potentiometer (Omega: LP8046) attached with brackets printed with a rapid prototyper. The components were mounted on a 20 mm thick 6061 aluminum plate with 40x40 mm bars bolted on each side to increase its stiffness. The trunnion mounts with plain bearings are used to align the actuator and damper and reduce the moment transmitted between the two. The linear actuator is fully integrated with a motor driver and provides 1090 counts per mm for position/velocity feedback via a quadrature encoder. The actuator was commanded with an analog ± 10 VDC position reference signal. The actuator can provide up to 5.5 kN, and move at up to 85 mm/s. The test bed is controlled with MATLAB Simulink Real-time Workshop which communicates via a National Instruments PCI-6229 data acquisition card.



Figure 22. Linear foot spring mechanism having independent stiffness values for plantar flexion and dorsiflexion in the linear domain.

Figure 22 shows a custom spring assembly acting as the linear foot. The assembly is 18 cm long and has a cross section of 7.5 cm by 7.5 cm; since the assembly is only to be used on the test bed apparatus, size was not a design constraint. The spring constant, k , is dependent on the sign of displacement, since an actual carbon fiber spring foot has a separate stiffness for its heel and toe. Table 5 gives the design requirements which are based on experimental data of a prosthetic foot used in all simulations, however the structural design allows the use of other springs of different stiffness. The layout of the sliding mechanism was designed to prevent binding, and incorporates low friction bushings. Dry graphite lubricant is also used to since the mechanism is open and wet lubricants would trap dirt.

TABLE 5. Design requirements for linear foot hardware

	k (N/mm)	Max Load (N)	Deflection (mm)
Toe	980	4000	4
Heel	288	1200	4

To control the damping coefficient of the damper, precise valve positions needed to be quickly achieved. To accomplish this, a PID controller was used in the Simulink program to track a reference valve angle, sending a voltage command to the servo valve driver (Advanced Motion Control: DZCANTE-020L080) controlling the current to the servo motor. Using the Zeigler-Nichols method, the PID gains were tuned to achieve a rise-time of less than 100 milliseconds for 90% and 0.5 degrees overshoot for a 90 degree command. To control the impedance of the valve, specific valve positions are used for open loop force control. This approach has far better performance than closed loop force feedback control since it has a much smaller phase lag, especially at higher frequencies [32].

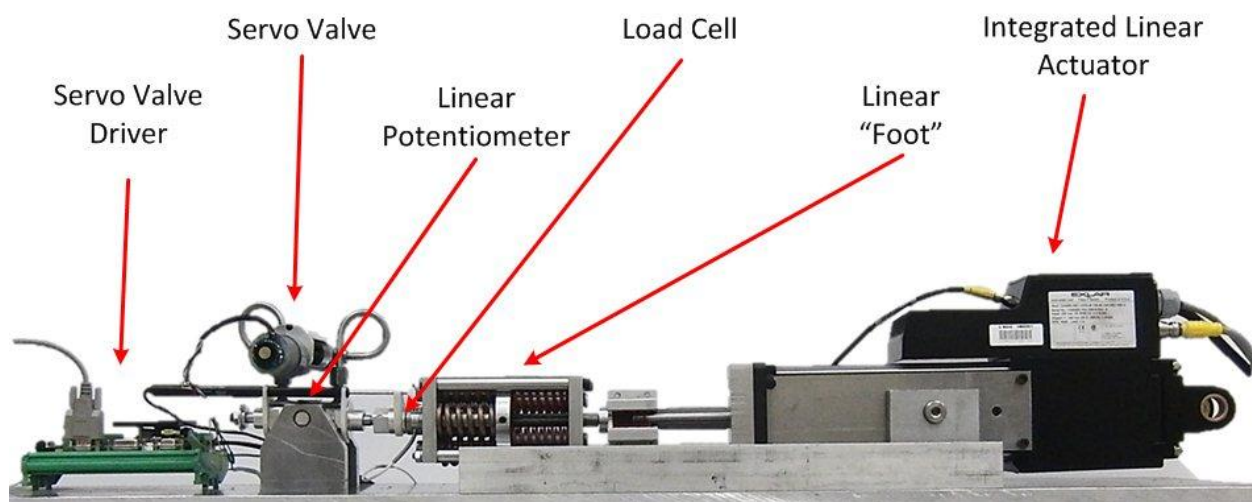


Figure 23. Test bed shown with key assemblies labeled.

To control the output of the linear actuator, it was given a reference command signal in the ± 10 VDC range proportional to either the position desired in reference to the home position, or in proportion to a desired velocity depending on which operational mode is chosen. Since the actuator is fully integrated, all tracking and closed loop control is done internally and is tunable.

The entire assembled test bed can be seen in figure 23 with all of the main sub-assemblies labeled.

5.4 Methods and Results

5.4.1 Characterization

In order to perform a hybrid simulation of the ankle, both the servo damper assembly and linear foot spring assembly needed to be characterized. To characterize the damper, the test bed was assembled without the linear foot and the force on the input rod was recorded at constant velocities. For valve positions from 5 to 90 degrees, the linear actuator was commanded at constant velocities of 2, 3, 5, 10, 20, 30, and 40 mm/s for both positive and negative directions. The resulting force and velocity from the load cell and actuator encoder respectively were recorded. For each valve position/actuator velocity condition, the force versus velocity was plotted. A least squares linear fit of points that each represented the average force and velocity for each constant velocity was taken, and the slope of these lines indicated the damping coefficient b , or force per velocity $b = F / \dot{x}$, at each valve position. This series of tests was performed five times and the mean damping coefficients and standard deviations were calculated. These mean damping coefficients can be seen in figure. 24, shown with an exponential fit having the form $b_{damping} = ae^{bx} + ce^{dx}$ that is used to calculate the valve position needed for a desired damping coefficient. It was observed that this type of data fit had the least error compared to other commonly used data fitting methods. Since the damping system operates bi-directionally, two exponential fits were calculated. The coefficients for the fits can be seen in Table 6. It can be seen that the fits closely resemble each other, and have similar coefficients. It is important to note that data below 10 degrees was extremely difficult to collect

for a number of reasons including high pressures, and difficulty to accurately position the servo valve. This is reflected in the standard deviation of the data collected. Since all tuning that is done takes place in positions greater than 10 degrees, it is justified that data below 10 degrees can be truncated for a more accurate exponential fit.

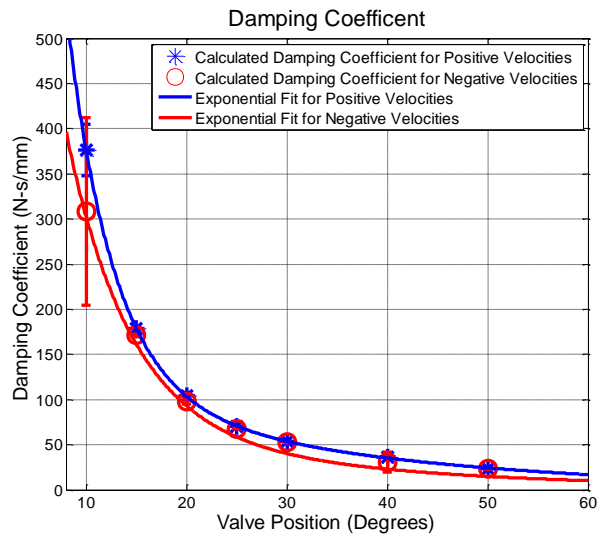


Figure 24. Damping coefficient in the tunable range for positive and negative velocities show with exponential fits.

TABLE 6 Exponential fit coefficients for positive and negative velocities.

Velocity	a	b	c	d
Positive	2365	-0.2160	148.7	0.0362
Negative	1162	-0.1574	88.77	0.0271

The servo valve needed to be characterized to account for backlash when tuning the damping coefficient. The servo attached to the valve has a 64 count hull effect encoder before the 29:1 gear box, yielding 1856 counts per revolution, or a resolution of about 0.2 degrees; however the backlash in the gearbox maximizes the resolution on the valve to about 1.2 degrees, which was measured with the encoder. The backlash is compensated for in the control.

The last two characterizations performed were the linear foot positive and negative stiffness, and the locked damper stiffness. This was performed by assembling the full test bed with the linear foot between the damper and linear actuator, locking the damper by closing the valve fully, and commanding the linear actuator to follow a triangular wave position trajectory. The recorded actuator position, actuator velocity, system force, and damper position can be seen in figure 25.

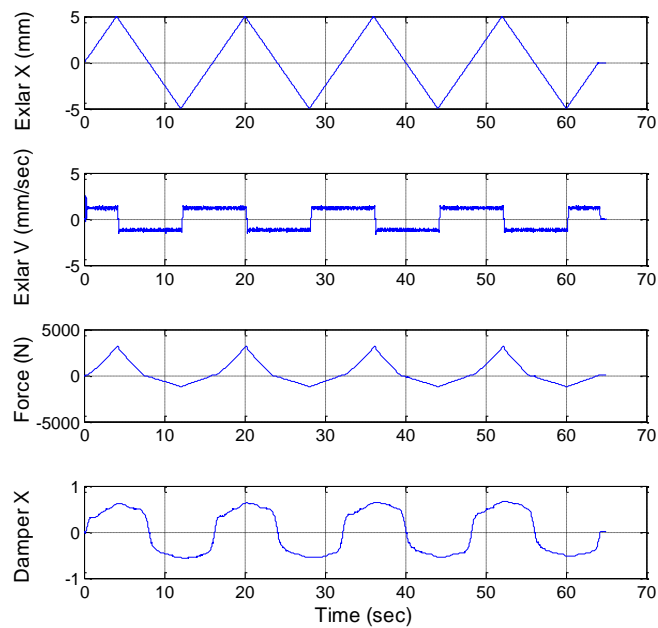


Figure 25. Recorded Exlar linear actuator position, actuator velocity, exerted force, damper position from top to bottom for damper and linear foot stiffness calculations.

To calculate the damper locked stiffness, the damper position was plotted against the force as seen in figure 26, and then broken up into 4 sections representing loading and unloading each for positive and negative loading as seen in figure 27. The mean least squares linear fit was calculated and taken to be the damper locked stiffness for each condition and can be seen in Table 7. A dead band of .8 mm indicating internal seal shift was also recorded to be accounted for during simulation.

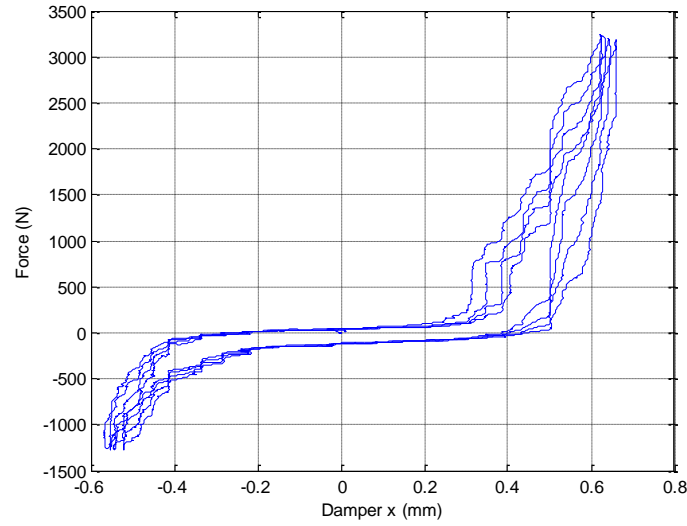


Figure 26. Damper position vs system force.

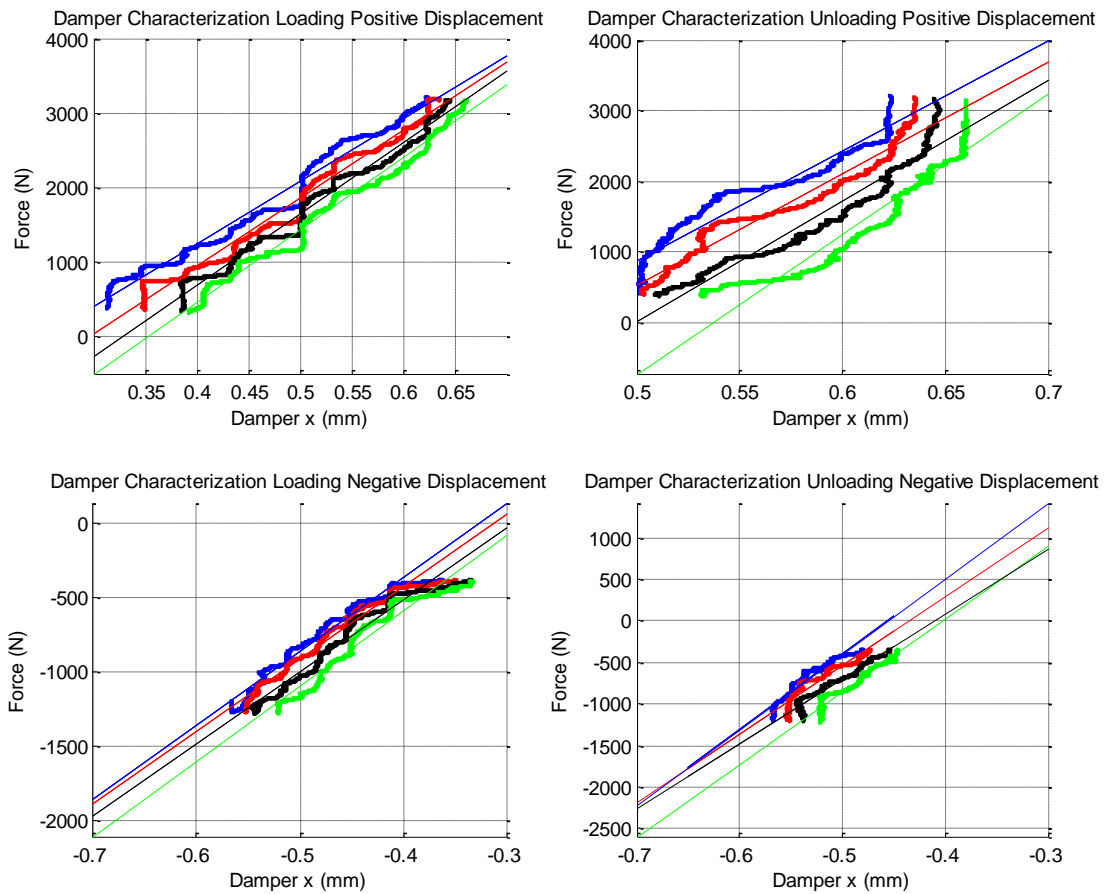


Figure 27. Loading and unloading phases for positive and negative displacement loading conditions for locked damper condition stiffness calculation.

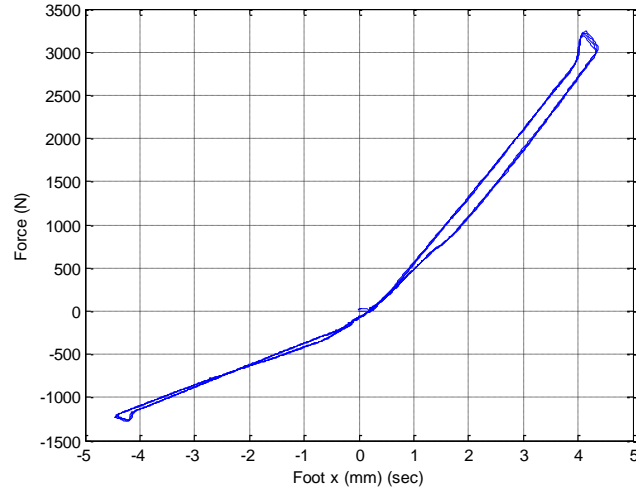


Figure 28. Linear foot deflection vs system force for foot stiffness calculations.

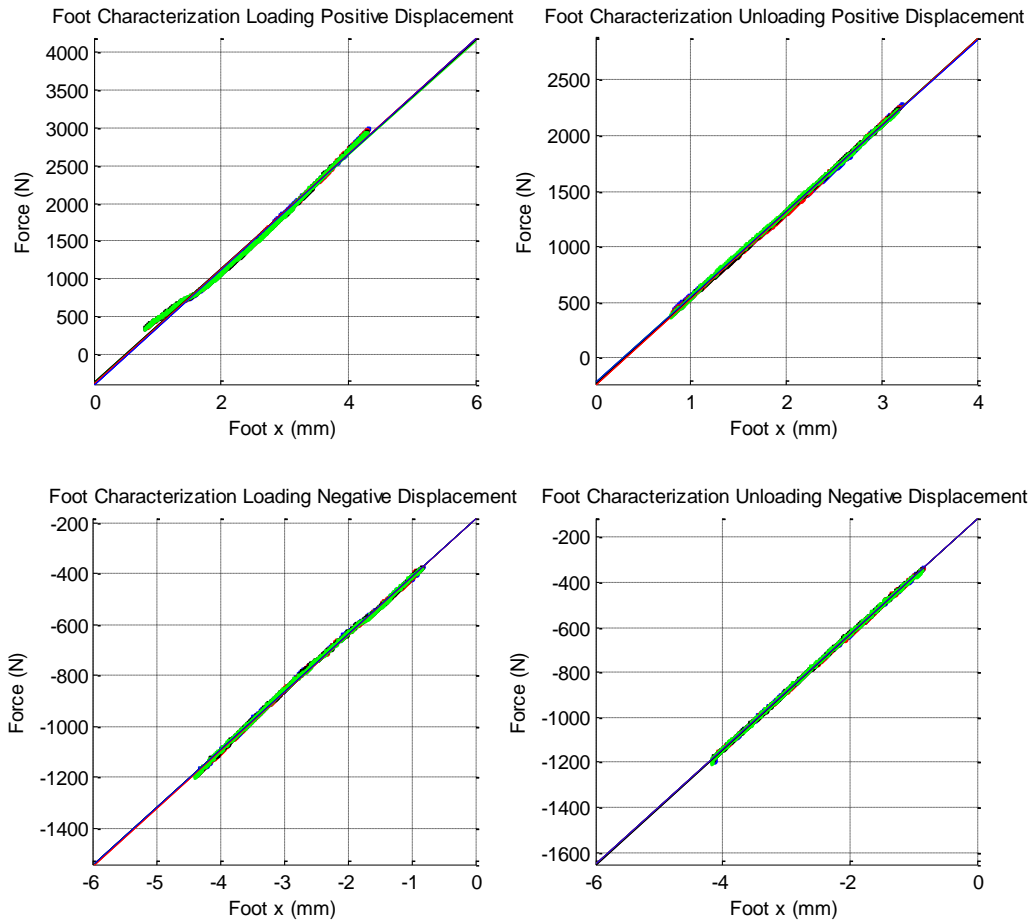


Figure 29. Loading and unloading phases for positive and negative displacement loading conditions for linear foot stiffness calculation.

To calculate the linear foot stiffness, the difference between damper and actuator stiffness was plotted against the system force as seen in figure 28 and then broken up into 4 sections representing loading and unloading each for positive and negative loading as seen in figure 29. The mean least squares linear fit was calculated and taken to be the damper locked stiffness for each condition and can be seen in Table 7.

TABLE 7 Average foot and locked damper stiffness used in hardware simulation

Linear Foot Stiffness (N/mm)			Damper Locked Stiffness (N/mm)		
	Loading	Unloading		Loading	Unloading
Positive Disp	755	773	Positive Disp	9216	17046
Negative Disp	226	256	Negative Disp	4950	8477

5.4.2 Hardware in the Loop Simulation

To simulate the adaptive prosthetic system the physical hardware (damper and linear foot) was used. In the adaptive ankle model

$$\theta_A = \frac{\tau_A}{k_f} + \int \frac{\tau_A - k_r \theta_d}{b} dt, \quad (7.1)$$

θ_A represents the total ankle angle from the combination of the spring and damper in series. The spring foot used in virtual simulations has a stiffness of 2.5 N-m/deg and 8.5 N-m/deg for the heel and toe, respectively. The ankle torque data, τ_A , was taken from an amputee wedge stepping study recorded in a previous study by the authors (presented in the Introduction and in more detail in [10]) and is used as the input, predicting the total ankle angle, θ_A , damper angle, θ_d , and spring angle, θ_s , scaled to accurately represent the characterized linear foot spring assembly. The total angle is converted into the linear domain using a 2.23 cm moment arm [2] in a slider crank geometry yields a linear damper reference position for the linear actuator to follow.

Throughout the gate cycle, the commanded damping coefficient is modified using previously tuned damping coefficients when motion is first detected, and at the angular velocity maxima and minima as done in previous work [1]. These are easily identified events that occur in all normal walking gate cycles such as heel strike or changes in the joint velocity direction. The characterized damper assembly stiffness, characterized linear foot stiffness, and associated damper stiffness dead band are used to generate the proper force on the damper assembly. To compensate for the bias in the loading caused by the locked damper dead band when internal seals are shifting a reference of 0.8 mm is added to the total joint position reference when the load on the damper reverses directions. This accounts for loading that occurs during virtual simulation, but not during the hardware simulation.

The recorded data from this test is the force on the damper, which is converted back to the rotational domain for comparison to the torque seen in a passive spring ankle prosthesis and a healthy able-bodied ankle for different initial steps (figure 30). The total adaptive ankle angle from the simulation for the same initial steps is also shown in figure 30 also compared to the passive and healthy ankle.

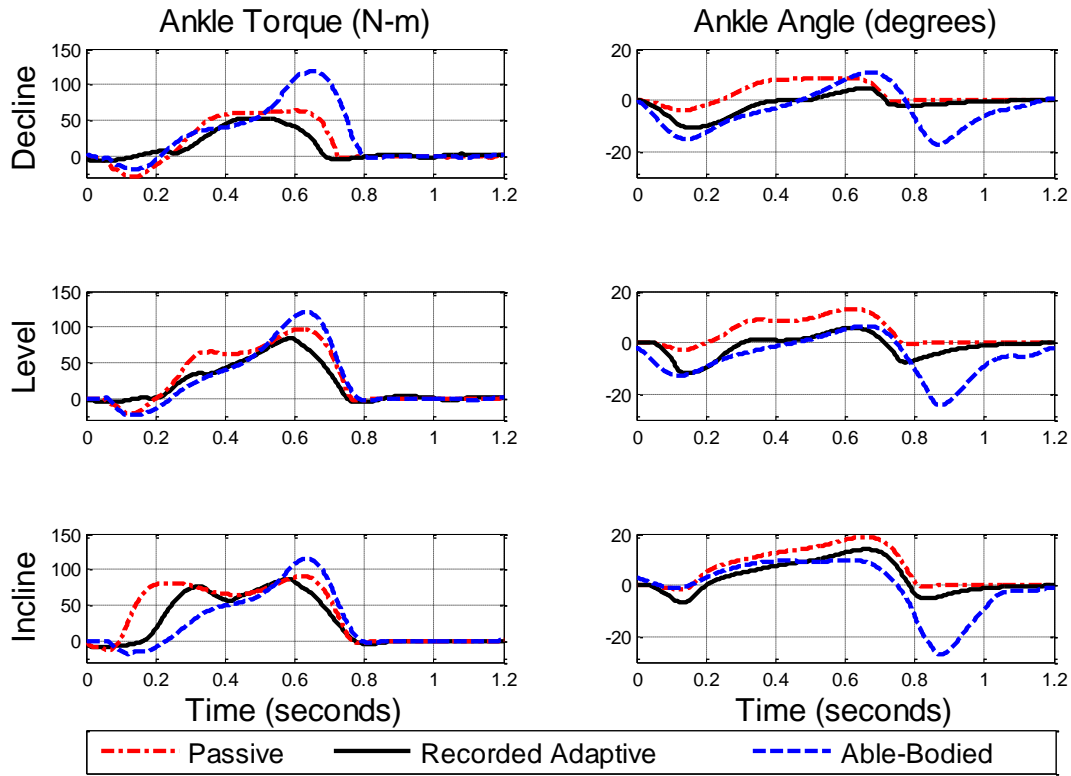


Figure 30. Ankle torque and angle for different initial steps showing the hybrid hardware in the loop adaptive simulation compared to able-bodied and passive amputee biomechanics data.

It is apparent that the recorded forces on the damper closely resemble the forces seen in a passive prosthesis, which is expected since the torque from the passive ankle prosthesis is used as an input to the system. When looking at the adaptive ankle angle in figure 30 however, it is seen that even though the torque of the adaptive ankle closely resembles that of the passive ankle prosthesis, the angular trajectory of the adaptive ankle is modified and better resembles that of a healthy ankle. This is evidence that through the dissipation of some energy by use of semi-active damping, stability in the amputees gate can be greatly improved.

5.5 Conclusion

The semi-active damping approach presented in this paper modulates the behavior of the ankle in real-time based on the characteristics of the forceful interaction between the ground, prosthesis, and amputee that encode the changes in terrain and user's activity. In this manner, a semi-active approach provides the advantages of a fully active system, but relies on the user-prosthesis interaction to enhance an amputee's stability throughout the gait cycle. Future work involves further development of the control algorithms, focusing on continuously modulating the damping coefficient during gait for improved performance. The result of this work will help in the development the adaptive prosthetic ankle to be tested in human subject trials

CHAPTER 6

THESIS CONTRIBUTIONS AND RECOMMENDATIONS

The main contribution that this work has to offer is strong evidence that semi-active damping technology has the potential to greatly improve walking conditions and stability for lower-limb amputees. This work will benefit not only the future development of intelligent prosthetics, but supports the potential to provide stability in mobile robotics.

Throughout the development and testing of this prototype, many things have been learned, bringing light to the difficulties of research projects and the importance of quality research techniques. The design of the damping system acted as it was designed to, however there are many things that arose from the design which inherently caused it to be very difficult to collect data from. The project encompassed many different disciplines leaving room for oversights that lead to the final conclusion that parts of this system need to be redesigned before being implemented in testing involving human subjects. Although this is the case, the information presented plays a valuable role in the future of semi-active damping systems in intelligent lower limb prostheses.

Among the problems encountered, air in the system was by far the most difficult to work around. A needle valve was chosen as the throttling device, and it was not realized until late in the project that as the valve opens, the volume of the damping system increases by a very small percentage. This creates a vacuum and draws a small amount of air into the system through either the valve seal or the rod seals. Once air gets into the system, it would create a slight spring in series with the damper effect, and the impedance produced by the damper would be shifted by displacement in proportion to the amount of the air in the system. The addition of air in the system wasn't instantaneous however, but would happen over a finite amount of time. This

allowed the opportunity to bleed the damping system in between tests in order to record accurate data. In future designs, a spool & sleeve valve should be designed and integrated into the damper housing. This type of valve maintains a constant system volume, takes incredibly low amounts of torque to operate, and is very compact. This makes it ideal for use in a damping system for an ankle prosthesis.

The process of bleeding the air out of the system highlighted the second most prominent design flaw. Bleeding the air out of the system takes a good amount of effort, and requires disassembly of a good portion of the test bed. The integration of a self-bleeding system would greatly improve the performance of the system as it would be much more consistent, and would require much less maintenance. Even if a different valve were used, air would most likely still get into the system. There are companies that have developed similar systems for knee prostheses that have reported if the device is stored upside down, air may potentially get into the system. In this event, it is documented that cycling the knee 15-20 times will cause the damper to self-bleed. It is now realized that in order to bring a system to commercial grade, such a system would be necessary. Even for the next generation prototype to be used for clinical trials, a self-bleeding system integrated into the damper is a must.

Another design change that is to be investigated is to have independent valves for dorsiflexion and plantar flexion. Having two valves offers two advantages over the current design. The first stems from the fact that the average working damping coefficient for dorsiflexion is different than that of plantar flexion. If two valves are used, the energy consumption will decrease since the valves will only be adjusting minutely every step, instead of having one valve closing and opening every step. The second advantage of having two valves is allowing the fluid to move in a constant direction through the constricted fluid paths of the

system, which is good for two reasons. Not having to change directions means that there is less fluid inertia needing to be overcome when switching joint velocity directions, which would improve the responsiveness when high impedance must be applied during these joint direction changes. The second benefit of having a constant fluid direction relates back to the second design flaw, which is lack of self-bleeding. The fluid moving in a constant direction means that any air taken into the system will be cycled completely and will be forced to go through the self-bleeding mechanism.

Other physical design changes that will be considered in the next generation prototype include port configuration of the cylinder, and sealing of the cylinder. At current, the bleeder ports are opposite of the fluid flow ports in the end caps. Future designs should have a single housing for the cylinder with one of the end caps machined out of the same billet. The other end cap should be sealed with an O-ring. The ports should be configured in pairs at each end of the cylinder but on the same face, and should also be sealed with O-rings. This port configuration allows ease of adaptability for throttling mechanisms, whether it is a spool & sleeve valve, or perhaps a prototype of a coiled throttle body for use with magneto-rheological fluid.

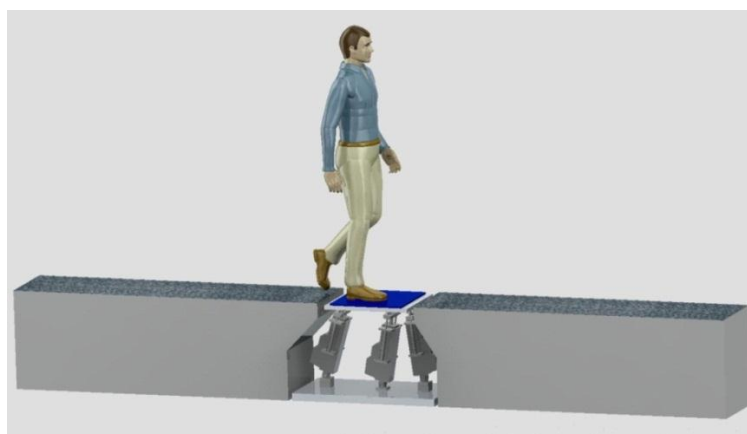


Figure 31. CAD model of dynamic joint impedance testing robot design.

Besides physical design changes to the semi-active damping system, it was realized throughout the testing process that a more fundamental understanding of the dynamic joint impedance of the human ankle must be understood in order to implement realistic impedance changes throughout the gait cycle when unexpected disturbances occur. There are many studies that have been conducted that test the static joint impedances of the healthy human ankle, however there has been little research done to test the dynamic impedance. It has been suggested in the literature that a robot should be designed to test this dynamic impedance. Figures 31 and 32 show a design of such a robot that will have the capability of testing this impedance. Having three linear actuators acting in line in parallel on a platform at floor level that a healthy subject can step on during normal walking can introduce a quick rotational perturbation around any joint of the leg in contact with the platform. Making use of this sudden movement, the dynamic joint impedance can be measured via a 3 dimensional video motion capture system and force platform mounted on the top of the robotic platform.

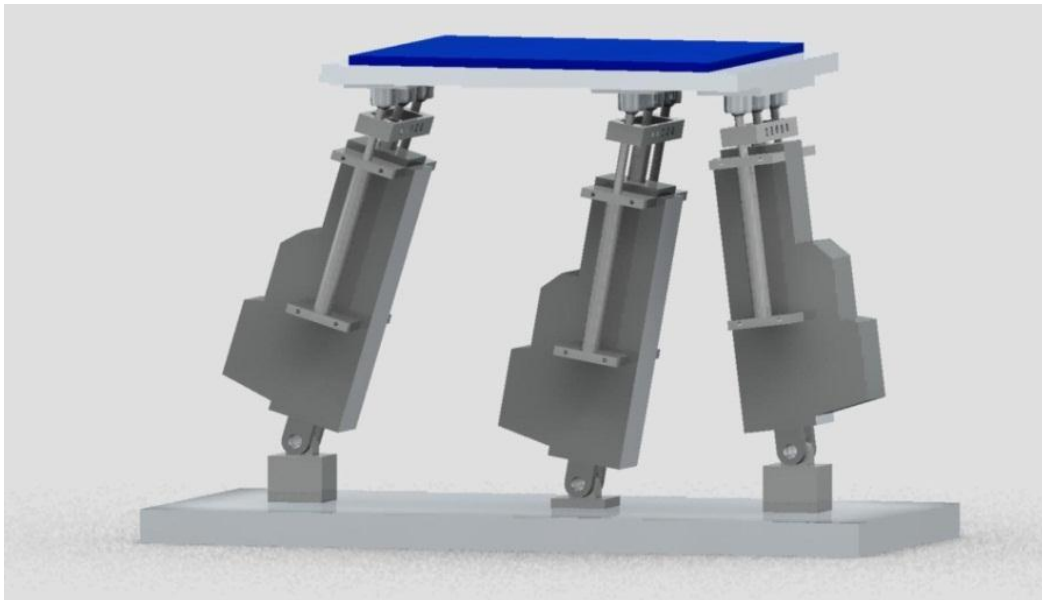


Figure 32. Close up of dynamic joint impedance testing robot

The end result of this thesis is valuable insight that will lead to a successful second generation prototype to be implemented in a clinical trial involving amputee test subjects. The end goal of the project has not changed, and remains as bringing this technology far enough to be commercialized in an actual transtibial prosthesis that will hopefully improve the living quality for transtibial amputees. .

BIBLIOGRAPHY

- [1] A. LaPre and F. Sup, "Simulation of a Slope Adapting Ankle Prosthesis Provided by Semi- Active Damping," *Mechanical Engineering*, pp. 587-590, 2011.
- [2] A. LaPre and F. Sup, "A Semi-Active Damper Design for use in a Terrain Adaptive Ankle Prosthesis," *2011 International Mechanical Engineering Congress and Exposition*, pp. 1-6, 2011.
- [3] D. A. Winter, *Biomechanics and motor control of human gait: normal, elderly and pathological*, 2nd ed. Waterloo, ON: University of Waterloo Press, 1991.
- [4] G. M. Earhart and a J. Bastian, "Form switching during human locomotion: traversing wedges in a single step.," *Journal of Neurophysiology*, vol. 84, no. 2, pp. 605-15, Aug. 2000.
- [5] D. H. Gates, J. Lelas, U. Della Croce, H. Herr, and P. Bonato, "Characterization of ankle function during stair ambulation.," *IEEE Engineering in Medicine and Biology Society Conference*, vol. 6, pp. 4248-51, Jan. 2004.
- [6] M. L. Palmer, "Sagittal plane characterization of normal human ankle function across a range of walking gait speeds," MS Thesis, Massachusetts Institute of Technology, Mechanical Engineering, 2002.
- [7] A. N. Lay, "Neuromuscular Coordination during Slope Walking," PhD Dissertatoin, School of Mechanical Engineering, Georgia Institute of Technology, 2005.
- [8] D. A. Winter and S. E. Sienko, "Biomechanics of below-knee amputee gait," *Journal of Biomechanics*, vol. 21, no. 5, pp. 361-367, 1988.
- [9] D. H. Gates, "Characterizing ankle function during stair ascent, descent, and level walking for ankle prosthesis and orthosis design," MS Thesis, Boston University, College of Engineering, 2004.
- [10] S. D. Prentice, E. N. Hasler, J. J. Groves, and J. S. Frank, "Locomotor adaptations for changes in the slope of the walking surface.," *Gait & Posture*, vol. 20, no. 3, pp. 255-65, Dec. 2004.
- [11] J. Gottschall and T. Nichols, "Neuromuscular strategies for the transitions between level and hill surfaces during walking," *Philosophical Transactions - Royal Society. Biological Sciences*, vol. 366, no. 1570, pp. 1565-1579, 2011.

- [12] R. S. Gailey and C.R. Clark, *Atlas of Amputations and Limb Deficiencies: Surgical, Prosthetic, and Rehabilitation Principles*. Rosemont, IL: American Academy of Orthopedic Surgeons, 2004, pp. 589-619.
- [13] A. H. Vrieling et al., "Uphill and downhill walking in unilateral lower limb amputees.," *Gait & Posture*, vol. 28, no. 2, pp. 235-42, Aug. 2008.
- [14] D. R. Vickers, C. Palk, a S. McIntosh, and K. T. Beatty, "Elderly unilateral transtibial amputee gait on an inclined walkway: a biomechanical analysis.," *Gait & posture*, vol. 27, no. 3, pp. 518-29, Apr. 2008.
- [15] C. Curtze, A. L. Hof, K. Postema, and B. Otten, "Over rough and smooth: Amputee gait on an irregular surface.," *Gait & Posture*, vol. 33, no. 2, pp. 292-296, Dec. 2011.
- [16] W. C. Miller, M. Speechley, and a B. Deathe, "Balance confidence among people with lower-limb amputations.," *Physical Therapy*, vol. 82, no. 9, pp. 856-65, Sep. 2002.
- [17] H. A. Mauch, "The development of artificial limbs for lower limbs.," *Bulletin of Prosthetics Research*, no. Fall, pp. 158-166, 1974.
- [18] R. J. Williams, A. H. Hansen, and S. A. Gard, "Prosthetic ankle-foot mechanism capable of automatic adaptation to the walking surface.," *Journal of Biomechanical Engineering*, vol. 131, no. 3, p. 035002, Mar. 2009.
- [19] F. Sup, H. A. Varol, J. Mitchell, T. J. Withrow, and M. Goldfarb, "Preliminary Evaluations of a Self-Contained Anthropomorphic Transfemoral Prosthesis.," *IEEE/ASME transactions on mechatronics : a joint publication of the IEEE Industrial Electronics Society and the ASME Dynamic Systems and Control Division*, vol. 14, no. 6, pp. 667-676, Jan. 2009.
- [20] R. D. Bellman, M. A. Holgate, and T. G. Sugar, "SPARKy 3: Design of an active robotic ankle prosthesis with two actuated degrees of freedom using regenerative kinetics," *2008 2nd IEEE RAS & EMBS International Conference on Biomedical Robotics and Biomechatronics*, pp. 511-516, Oct. 2008.
- [21] S. Au, M. Berniker, and H. Herr, "Powered ankle-foot prosthesis to assist level-ground and stair-descent gaits.," *Neural networks : the official journal of the International Neural Network Society*, vol. 21, no. 4, pp. 654-66, May. 2008.
- [22] A. N. Lay, C. J. Hass, and R. J. Gregor, "The effects of sloped surfaces on locomotion: a kinematic and kinetic analysis.," *Journal of Biomechanics*, vol. 39, no. 9, pp. 1621-8, Jan. 2006.
- [23] Nillic, "Amputation Statistics by Cause Limb Loss in the United States Amputation Statistics by Cause Limb Loss in the United States.," *Physical Medicine and Rehabilitation*, pp. 1-3, 2008.

- [24] K. Ziegler-Graham, E. J. MacKenzie, P. L. Ephraim, T. G. Travison, and R. Brookmeyer, "Estimating the prevalence of limb loss in the United States: 2005 to 2050.," *Archives of Physical Medicine and Rehabilitation*, vol. 89, no. 3, pp. 422-9, Mar. 2008.
- [25] W. C. Miller, a B. Deathe, M. Speechley, and J. Koval, "The influence of falling, fear of falling, and balance confidence on prosthetic mobility and social activity among individuals with a lower extremity amputation.," *Archives of Physical Medicine and Rehabilitation*, vol. 82, no. 9, pp. 1238-44, Sep. 2001.
- [26] J. Kulkarni, S. Wright, C. Toole, J. Morris, and R. Hirons, "Falls in Patients with Lower Limb Amputations: Prevalence and Contributing Factors," *Physiotherapy*, vol. 82, no. 2, pp. 130-136, Feb. 1996.
- [27] H. A. Mauch, "Control mechanism for artificial ankle," U.S. Patent 2,843,853 1958.
- [28] R. J. Williams, A. H. Hansen, and S. A. Gard, "Prosthetic ankle-foot mechanism capable of automatic adaptation to the walking surface," *Journal of Biomechanical Engineering*, vol. 131, no. 3, p. 035002, Mar. 2009.
- [29] R. O. N. Seymour et al., "Comparison between the C-leg 1 microprocessor-controlled prosthetic knee and non-microprocessor control prosthetic knees : A preliminary study of energy expenditure , obstacle course performance , and quality of life survey," *Physical Therapy*, vol. 31, no. March, pp. 51 - 61, 2007.
- [30] K. R. Kaufman et al., "Gait and balance of transfemoral amputees using passive mechanical and microprocessor-controlled prosthetic knees," *Gait & Posture*, vol. 26, pp. 489-493, 2007.
- [31] D. R. Vickers, C. Palk, a S. McIntosh, and K. T. Beatty, "Elderly unilateral transtibial amputee gait on an inclined walkway: A biomechanical analysis.," *Gait & Posture*, vol. 27, no. 3, pp. 518-29, Apr. 2008.
- [32] D. J. C. F.H. Besinger, D. Cebon, "Force control of a semi-active damper Title," *Vehicle System Dynamics*, no. 24, pp. 695-723, 1995.